7-2008

β-Diketonate, β-Ketoiminate, and β-Diiminate Complexes of Difluoroboron

Felipe P. Macedo
Marquette University

Chengeto Gwengo
Marquette University

Sergey Lindeman
Marquette University, sergey.lindeman@marquette.edu

Mark D. Smith
University of South Carolina

James R. Gardinier
Marquette University, james.gardinier@marquette.edu

European Journal of Inorganic Chemistry, Vol. 2008, No. 20 (July 2008): 3200-3211. DOI.

β-Diketonate, β-Ketoiminate, and β-Diiminate Complexes of Difluoroboron

Felipe P. Macedo
Department of Chemistry, Marquette University, Milwaukee, WI
Chengeto Gwengo
Department of Chemistry, Marquette University, Milwaukee, WI
Sergey V. Lindeman
Department of Chemistry, Marquette University, Milwaukee, WI
Mark D. Smith
Department of Chemistry and Biochemistry, University of South Carolina, Columbia, SC
James R. Gardinier
Department of Chemistry, Marquette University, Milwaukee, WI

Abstract

A series of β-diketonate, keto(aryl)iminato, and β-bis(aryl)iminato complexes of difluoroboron, twenty in total, have been prepared to assess the impact of chelate ring and aniline substitution on the structural, electrochemical, and photophysical properties of these ubiquitous chelates. DFT (B3LYP/6-

31G*) calculations supplemented the experimental results and both demonstrated that replacing oxygen with the more electron-donating aniline groups serves to only fine-tune the electronic properties because both the HOMO and LUMO energies are affected by such substitution. The electronic properties of all compounds are most greatly influenced by the nature of the substituents bound to the carbon portion of the chelate ring. Each difluoroboron complex undergoes two ligand-based, one-electron reductions where the first reduction potential becomes less favorable with increasing aniline substitution. Similarly, replacing oxygen with the more electron-donating aniline groups gives rise to slightly red-shifted absorption and emission processes. Substitution on the aniline ring has little, if any, influence on the electronic properties of the resultant complexes.

Abstract

A series of β-diketonate, β-ketoiminate, and β-diiminate complexes of difluoroboron have been prepared to evaluate the effects of chelate ring substitution on the structural and electronic properties. The electron-accepting nature of the ligands likely facilitates unusual coordination chemistry.

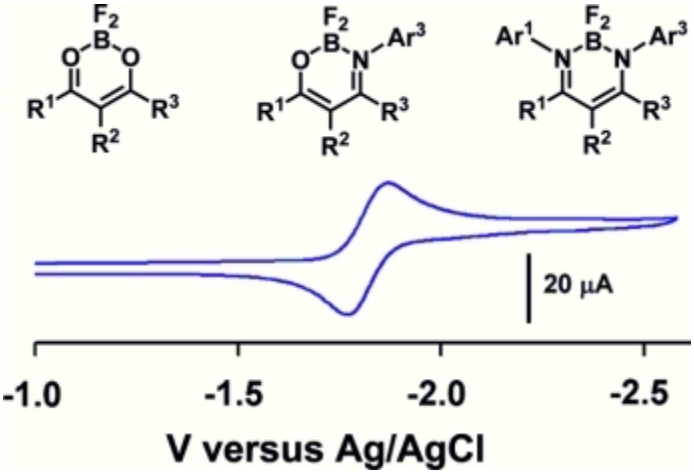

Introduction

There is a long-standing interest in β-diketonato and related chelate complexes (Figure 1) of main group and transition metals for both fundamental studies and a myriad of practical applications.1 Recent success in utilizing sterically-demanding β-diiminate ligands to stabilize unusual transition2 and main-group3 metal complexes has spurred resurgent interest in this class of chelates. Important for both applied and fundamental coordination chemistry studies is knowledge of the electronic properties of the ligands in their chelated forms. Such information permits assessment of the extent to which the ligands may serve either as true spectator ligands or as “non-innocent” electron reservoirs, offering new possibilities for (often unanticipated) reaction chemistry. For this purpose, studies of complexes whose Lewis acid centers are electrochemically silent are critical for evaluating the potential for the ligand to remain non-innocent.

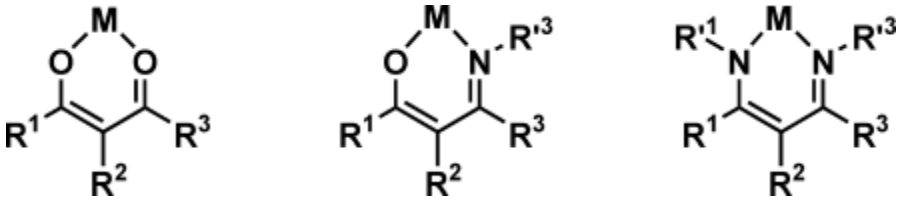

Figure 1. From left to right: β-diketonato, β-ketoiminato, and β-diiminato chelate complexes. M = metal or metalloid; R^1, R^3 = organyl; R^2, $R^{1\prime}$, $R^{3\prime}$ = H, or organyl.

The difluoroboron moiety is one Lewis acid particularly well-suited for such studies, especially because the known β-diketonato, β-ketoiminato, and β-diiminato complexes[4–6] are reported to be air-stable and, in some cases, interesting reaction chemistry,[7] electrochemistry,[8] photochemistry,[9] and luminescence behavior have been reported.[10] We were interested in incorporating β-ketoiminato and β-diiminato chelates of difluoroboron and of metals as functional "sensing" groups in molecular assemblies and for the stabilization of low-oxidation state species.[11] While detailed studies on the photophysics of fluorescent and phosphorescent behavior as well as of exciplex formation involving difluoroboron diketonate derivatives are available,[9–10] detailed reports concerning the electronic properties of β-ketoiminato, and β-diiminato derivatives were not, to the best of our knowledge. For this purpose, it became necessary to learn whether the interesting electronic properties found in the diketonates were retained in the β-ketoiminato and β-diiminato derivatives. If so, we wanted to assess the impact of substitution on the "tunability" of the photo- and electrochemical properties of such systems. To this end, we report now on our findings regarding the structural and electronic properties of a series of diketonato, ketoiminato, and diiminato complexes of difluoroboron. Also, in an effort to make comparisons between the different ligands more intuitive, we will introduce the following non-standard shorthand notation, ($R^{1R'1}$,R^2,$R^{3R'3}$), with reference to Figure 1. The presence of two superscripts ($^{R'1}$ and $^{R'3}$) refers to a β-diiminate, the presence of only one superscript ($^{R'1}$ or $^{R'3}$) refers to a β-ketoiminate, whereas the absence of superscripts implies a β-diketonate. Thus, the hypothetical free ligand and BF_2 complex in Figure 2a and Figure 2b, respectively, would be designated as $H(CH_3,H,CF_3^{m\text{–}(OMe)C6H4})$ and $BF_2(t\text{Bu}^{Dipp},Et,\text{Me}^{n\text{Bu}})$ according to the above shorthand notation. The substituent priority follows from the usual order for donor heteroatoms (O > N), then organyls with ($R^{1\prime}/R^{3\prime}$) > (R^1/R^3).

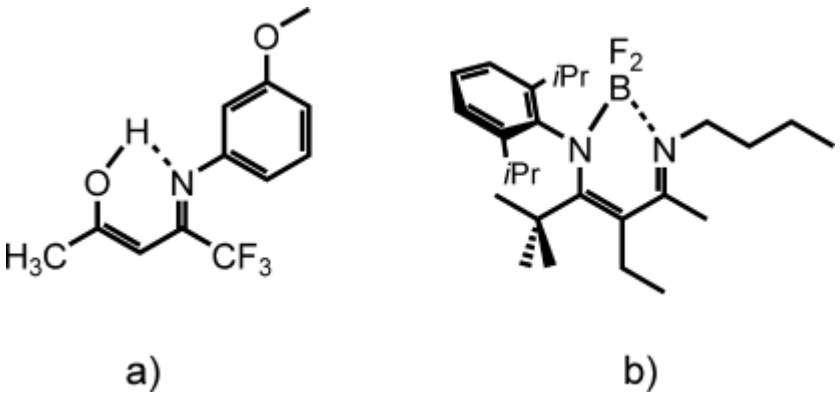

Figure 2. Hypothetical (a) free ligand $H(CH_3,H,CF_3^{m\text{-}(OMe)C6H4})$ and (b) difluoroboron complex $BF_2(t\text{Bu}^{Dipp},Et,\text{Me}^{n\text{Bu}})$ Dipp = diisopropylphenyl.

Results and Discussion

Synthesis

The difluoroboron chelates that were prepared in this study are listed in Table 1 and several details of the syntheses are worth noting. First, while most of the diketones are commercially available, the triphenyl diketone, H(Ph,Ph,Ph) is not. Of the several literature methods for the preparation of this compound,[12] we found that the ozonolysis of tetraphenylcyclopentanedione[12a] was, by far, the simplest and the most reliable route. Most of the ketoiminates and some of the diiminates could be prepared by acid-catalyzed condensation reactions between the diketones and anilines (Scheme 1). For derivatives originating from the unsymmetrical benzoylacetone, H(Ph,H,Me), NMR studies show substitution first occurs at the acetyl portion of the chelate and then, slowly, and with lower yields, the second substitution occurs at the benzoyl portion. This observation is in agreement with the known lower reactivity of aryl- vs. aliphatic ketones. In this vein, we were unable to prepare β-diiminato derivatives of the 1,3-diaryl diketones, H(Ph,H,Ph), H(Ph,Ph,Ph), and H(4-MeOC$_6$H$_4$,H,4-MeOC$_6$H$_4$) by acid condensation; the second condensation step did not occur even after prolonged heating, or with higher reaction temperatures, or even when using concentrated HCl as a catalyst. Apparently, the already low reactivity of 1,3-diaryl diketones is significantly further diminished upon initial substitution of the electron-donating aniline substituent. Similarly, all attempts to obtain H(*t*Bu,H,*t*Bu^{Ph}) and H(*t*Bu^{Ph},H, *t*Bu^{Ph}) with *tert*-butyl groups on the chelate ring, by acid-catalyzed condensation failed to provide any of the desired products; presumably steric considerations inhibit the reaction as the starting materials are fully recovered. Thus, H(*t*Bu,H,*t*Bu^{Ph}) and H(*t*Bu^{Ph},H,*t*Bu^{Ph}) were prepared by a known multi-step route (Scheme 2).[13,14] Finally, the difluoroboron complexes were prepared by the straightforward HF elimination reaction in toluene, where the evolved HF (which did not appear to interfere with the reaction pathway) was passed into a 1 M KOH scrubbing solution.

Table 1. Difluoroboron chelate complexes prepared in this study.

β-Diketonate	**β-Ketoiminate**	**β-Diiminate**
BF$_2$(*t*Bu,H,*t*Bu)	BF$_2$(*t*Bu,H,*t*Bu^{Ph})	BF$_2$(*t*Bu^{Ph},H,*t*Bu^{Ph})
BF$_2$(Me,H,Me)	BF$_2$(Me,H,Me^{4BrPh})	BF$_2$(Me^{4BrPh},H,Me^{4BrPh})
BF$_2$(Ph,H,Me)	BF$_2$(Ph,H,Me^{4BrPh})	BF$_2$(Ph^{4BrPh},H,Me^{4BrPh})
BF$_2$(Ph,H,Ph)	BF$_2$(Ph,H,Ph^{Ph})	
	BF$_2$(Ph,H,Ph^{2BrPh})	
	BF$_2$(Ph,H,Ph^{4BrPh})	
	BF$_2$(Ph,H,Ph^{2Br4Tolyl})	
	BF$_2$(Ph,H,Ph^{4pzPh})	
	BF$_2$(Ph,H,Ph^{2pz4Tolyl})	
BF$_2$(Ph,Ph,Ph)	BF$_2$(Ph,Ph,Ph^{4BrPh})	
BF$_2$(*p*Anis, H, *p*Anis)	BF$_2$(*p*Anis, H, *p*Anis^{4BrPh})	*p*Anis = 4-MeOC$_6$H$_4$

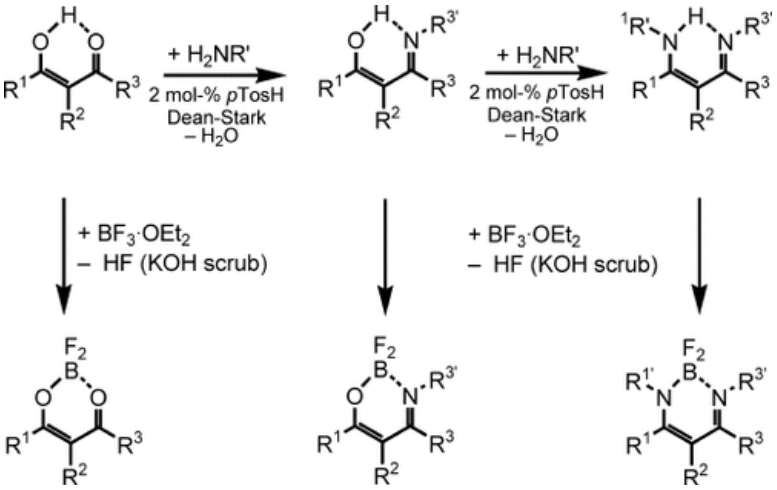

Scheme 1. Preparation of the β-ketoiminate and β-diiminate ligands by acid-catalyzed condensation, and of difluoroboron chelate complexes by HF elimination.

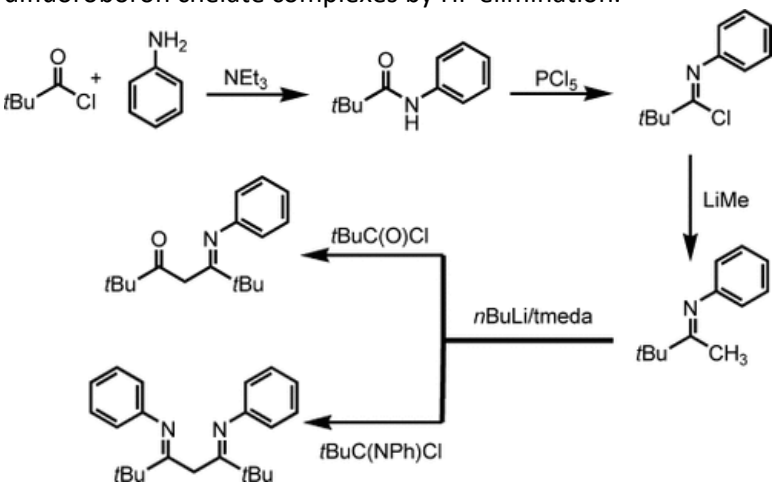

Scheme 2. Preparative route to β-ketoimino and β-diimine derivatives H(*t*Bu,H,*t*Bu^{Ph}) and H(*t*Bu^{Ph},H,*t*Bu^{Ph}).

The difluoroboron complexes are all air-stable. Those with aliphatic groups on the chelate ring are colorless while those with two aryl groups on the chelate ring are yellow. Moreover, derivatives with aliphatic groups on the chelate ring are soluble in most ethereal, aromatic, and halocarbon solvents, are modestly soluble in hot hexanes and alcohols, but are only slightly soluble in cold hexanes or pentane. The solubility of the derivatives decreases with increasing number of aromatic groups such that the diphenyl diketone derivatives are insoluble in hot hexanes.

Solid-State Structures

A total of twelve new difluoroboron chelate derivatives have been structurally characterized. The molecular structures of a representative β-diketonate, β-ketoiminate, and β-diiminate are given in Figure **3** while those of the remaining derivatives are found in the Supporting Information. Selected features of the intramolecular geometry of each derivative prepared in this study and of some previously known derivatives are provided in Table **2**. As expected, the B–N bonds (1.567 Å average) are about 0.1 Å longer than the B–O bonds (1.467 Å average). Thus, on traversing the series of diketonate, ketoiminate and diiminate complexes, the BF_2 group is displaced further away from the chelate ring and the FBF angle becomes more acute. The pertinent metrical parameters for the ensuing discussion of NMR spectroscopic data are the average BE_2 distance (E = N or O) and FBF angle of 1.483

Å and 110.7° for the diketonates, 1.518 Å and 110.4° for the ketoiminates, and 1.541 Å and 107.7° for the diiminates. Analysis of bond lengths in the ketoiminates suggests that the major resonance contribution to bonding is the alkoxy-imine form (Scheme **3**, left).

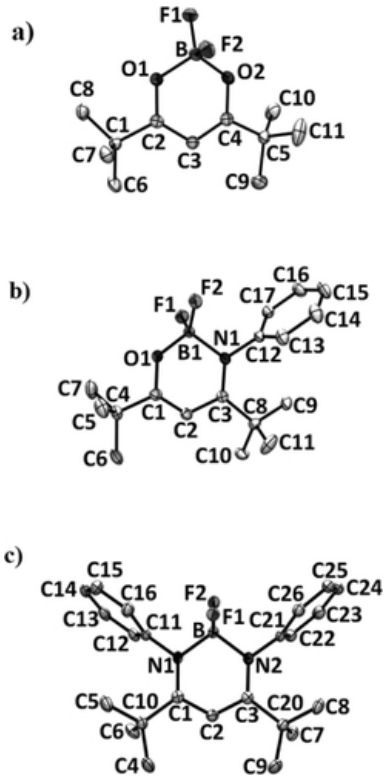

Figure 3. ORTEP diagrams of (a) BF_2(*t*Bu,H,*t*Bu), (b) BF_2(*t*Bu,H,*t*Bu^{Ph}), and (c) BF_2(*t*Bu^{Ph},H,*t*Bu^{Ph}). Hydrogen atoms removed for clarity. Ellipsoids are shown at 50 % probability level.

Table 2. Selected features of intramolecular geometry of some structurally characterized difluoroboron chelates.

Compound	B–O	B–N	C–O	C–N	C=C (O)	C=C (N)	B–Pl$_C$[a]	EBE	EBE-Pl$_C$	Pl$_C$-aryl dihedral[b]
	[Å]	[Å]	[Å]	[Å]	[Å]	[Å]	[Å]	[°]	[°]	[°]
Diketonate[g]										
BF_2(Me,H,Me)[c]	1.475	–	1.287	–	1.358	–	0.142	111.10	9.41	–
BF_2(*t*Bu,H,*t*Bu)	1.490	–	1.302	–	1.388	–	0.378	109.47	25.38	–
BF_2(Me,H,Ph)[d]	1.487	–	1.305	–	1.387	–	0.00	111.47	0.00	0.00
BF_2(Ph,H,Ph)[e]	1.483	–	1.294	–	1.380	–	0.251	110.97	17.05	3.69
BF_2(*p*Anis,H, *p*Anis)[f]	1.481	–	1.309	–	1.385	–	0.00	111.80	0.00	2.36
Ketoiminate										
BF_2(Me,H,Me^{4BrPh})	1.466	1.566	1.318	1.318	1.363	1.418	0.226	109.86	14.65	73.73
BF_2(*t*Bu,H,*t*Bu^{Ph})	1.458	1.579	1.321	1.322	1.360	1.427	0.368	109.53	24.47	85.33
	1.457	1.588	1.322	1.318	1.362	1.426	0.371	109.39	24.52	84.99
	1.450	1.577	1.317	1.318	1.358	1.430	0.182	110.77	11.40	75.29
BF_2(Ph,H,Ph^{Ph})	1.457	1.563	1.314	1.324	1.360	1.408	0.283	109.74	18.66	14.75, 52.91, 65.04
BF_2(Ph,H,Ph^{4BrPh})	1.460	1.569	1.316	1.318	1.365	1.408	0.067	110.14	4.32	11.18, 52.95, 64.53
BF_2(Ph,H,Ph^{2BrPh})	1.465	1.559	1.314	1.324	1.375	1.413	0.246	109.79	15.97	13.54, 54.26, 81.79
BF_2(Ph,H,Ph^{4pzPh})	1.469	1.564	1.312	1.322	1.367	1.415	0.084	110.37	5.52	1.24, 51.48, 76.12
	1.469	1.568	1.318	1.320	1.368	1.414	0.087	110.56	5.82	6.03, 64.84, 61.20
BF_2(Ph,H,Ph^{2pztol})	1.473	1.570	1.321	1.330	1.368	1.412	0.339	109.04	21.80	13.98, 43.76, 76.22
BF_2(Ph,Ph,Ph^{4BrPh})	1.464	1.572	1.319	1.318	1.383	1.428	0.108	108.93	6.81	32.70, 81.83, 80.66, 65.94
BF_2(*p*Anis,H,*p*Anis^{BrPh})	1.477	1.572	1.320	1.338	1.378	1.403	0.387	109.63	25.45	12.40, 39.75, 58.88
Diiminate[g]										
BF_2(Me^{Me},H,Me^{Me})[h]	–	1.523	–	1.326	–	1.384	0.000	110.18	0.00	–
BF_2(Me^{Me},H,Me^{iPr})[i]	–	1.534	–	1.331	–	1.387	0.238	110.42	15.37	–
BF_2(Me^{ptol},H,Me^{ptol})[j]	–	1.552	–	1.344	–	1.393	0.147	108.62	9.19	76.13
BF_2(Me^{4BrPh},H,Me^{4BrPh})	–	1.544	–	1.337	–	1.393	0.000	108.99	0.00	86.77
BF_2(*t*Bu^{Ph},H,*t*Bu^{Ph})	–	1.550	–	1.340	–	1.395	0.399	109.41	25.92	88.01, 86.57

[a] Pl$_c$ = Mean plane of E_2C_3 chelate ring; E = N,O as appropriate.

[b] Given in the order R^1, R^3, $R^{3'}$, R^2, see Figure 1 for labelling.

[c] CSD IHEDUU ref.15

[d] CSD BZACBF ref.16

[e] CSD XOCJOO ref.18

[f] CSD SANKUO ref.19
[g] Average values.
[h] CSD JENLOD ref.20
[i] CSD YALLIH ref.21
[j] CSD BOHFUZ ref.17

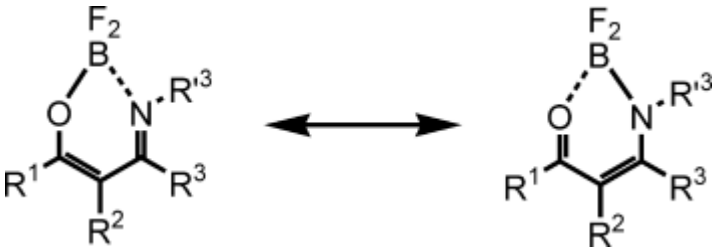

Scheme 3. Possible resonance forms for difluoroboron β-ketoiminates.

That is, for the complete series of difluoroboron chelates derived from either the parent acetylacetone (Me,H,Me)and 4-bromoaniline or tetramethylheptanedione (*t*Bu,H,*t*Bu)and aniline, the B–O bonds are shorter in the ketoiminate than in the corresponding diketonate while the B–N distance is longer in the ketoiminate than the average found in the analogous diiminate. These observations suggest that, in the ketoiminate, the B–N rather than the B–O interaction is dative in nature. Analysis of bond length alternations along the ketoiminate chelate backbone further supports such an assessment. As one example, the C–C bond on the keto side of the ring is significantly (ca. 0.04 Å) shorter than the C–C bond on the imine side, as might be expected from the resonance form on the left of Scheme **3**. Substitution on the aniline ring has very little, if any, impact on the bond lengths within the six-membered chelate ring. Interestingly, the chelate ring is often (but not always) distorted from planarity giving a half-boat conformation brought about by folding the E–B–E (E = N or O, as appropriate) moiety along the E···E hinge axis, affording "axial" and "equatorial" B–F bonds. The B–F bond lengths vary without a length prejudice when in axial or equatorial position and average 1.38 Å. The chelate ring puckering (measured by perpendicular distance from boron to the mean E_2C_3 chelate ring, Pl_C, or by the dihedral of the mean plane of the E–B–E group and Pl_C, Table **2**) appears to be a function of the crystal packing arrangement, as there is no clear correlation between electronic or intramolecular steric considerations of R^1, $R^{1\prime}$, R^3, $R^{3\prime}$ groups. This is particularly evident from the seemingly capricious nature of ring-puckering in the series of chelates derived from dibenzoylmethane (Ph,H,Ph) and triphenyl diketone (Ph,Ph,Ph). In fact, detailed analysis of crystal-packing interactions show that the BF_2 moiety is always involved in weak CH–F non-covalent interactions,**22** where the number and nature of the interactions depend, of course, on the types of groups present along the chelate periphery. In general, fluorines with more intermolecular noncovalent interactions have longer B–F bonds than more innocent fluorines.

NMR Spectroscopic Studies

With the possible exception of ketoiminates with *ortho*-aniline substitution (to be discussed later), the ^{11}B and ^{19}F NMR (and to a lesser extent the ^{1}H and ^{13}C), spectroscopic data (Figure **4**) reveal that the difluoroboron chelates generally achieve more symmetric conformations in solution compared to the static solid-state ring-puckered structures, but no dynamic processes could be detected for any chelate over the temperature range 213–373 K. This observation is particularly evident since complexes with symmetrically equivalent fluorines (derivatives with planar chelate rings, or those with exchange-averaged solution structures due to fast ring-flipping processes, etc.) are expected to have only one triplet ^{11}B NMR resonance near 0 ppm indicative of symmetric tetracoordinate boron**23** and a single quartet resonance [with a satellite septet resonance from the 18.8 % naturally-abundant ^{10}B (I = 3) isotope] in the ^{19}F NMR spectrum. On the other hand, static ring-puckered structures as found in most of the solid-state structures (Table **1**), would impose symmetric inequivalence of fluorines, and two sets of doublet resonances (for B–F coupling) would be anticipated in the ^{11}B spectrum. In this scenario, the ^{19}F NMR spectrum would be expected to consist of two sets of doublet-of-quartet resonances for each type of fluorine, due to both geminal F–F coupling and to one-bond ^{11}B–^{19}F coupling (with appropriate satellites resonances for ^{10}B–^{19}F coupling). For most of the compounds, the former (symmetric) case applies, demonstrated by the spectra of BF_2(Ph,H,Ph^{4BrPh}) shown in part A of Figure **4**. As illustrated in Figure **4**(B) for BF_2(Ph,H,Ph), the spectra of the diketonates are unusual in that the expected B–F coupling is not observed presumably due in part to fast relaxation of the

quadrupolar boron nucleus,[24] and, in part, due to the unusual nature of the diketonates (vide infra). For ketoiminates with (asymmetric) *ortho*-aniline substitution, the fluorines are symmetrically inequivalent and more complex spectra are observed in accord with the above discussion and as seen in the spectra of BF_2(Ph,H,Ph^{2BrPh}), Figure 4 (C). For such asymmetric cases, the F–F geminal coupling constant is generally about 90 Hz while the disparate B–F coupling constants of about 20 Hz (for the resonance near δ = –130 ppm), and 8 Hz (for the resonance near δ = –142 ppm) further emphasize the difference in the environments about each fluorine. It was not possible to access a more symmetric conformation, even on heating to 373 K. It is noteworthy that for the twenty compounds studied here, unexpected trends in the ^{19}F chemical shift and the magnitude of the $J_{B–F}$ coupling constant are observed. For the diketonate complexes, the average ^{19}F chemical shift and $J_{B–F}$ coupling constant are δ_F = –139.6 with $J_{B–F}$ ca. 0 Hz while the average values for the ketoiminate and diiminate complexes are δ_F = –135.0, $J_{B–F}$ = 15 Hz and δ_F = –131.2, $J_{B–F}$ = 29 Hz, respectively. Normally, one expects the chemical shift and the magnitude of the scalar coupling to increase with increasing electronegativity of groups bound to boron (increasing the s-character of the B–F bond). We tentatively attribute this unusual behavior to the differences in shielding caused by the magnetic anisotropy associated with the ring currents above and below the chelate rings. The structural studies indicate that the BF_2 group is closest to the chelate ring with the most obtuse FBF angle, allowing the fluorines (above and below the plane of the chelate ring) to penetrate more deeply into the ring currents compared to the ketoiminate and the diiminate complexes with fluorines that are progressively located further away from the chelate ring; the fluorines of the diketonate complexes are most shielded, followed in order by those on the ketoiminate and diiminate complexes. The trend in magnitude of the B–F coupling constants may then be reconciled if the increased shielding effectively makes the fluorines “lesselectronegative” than in the absence of the chelate ring currents.

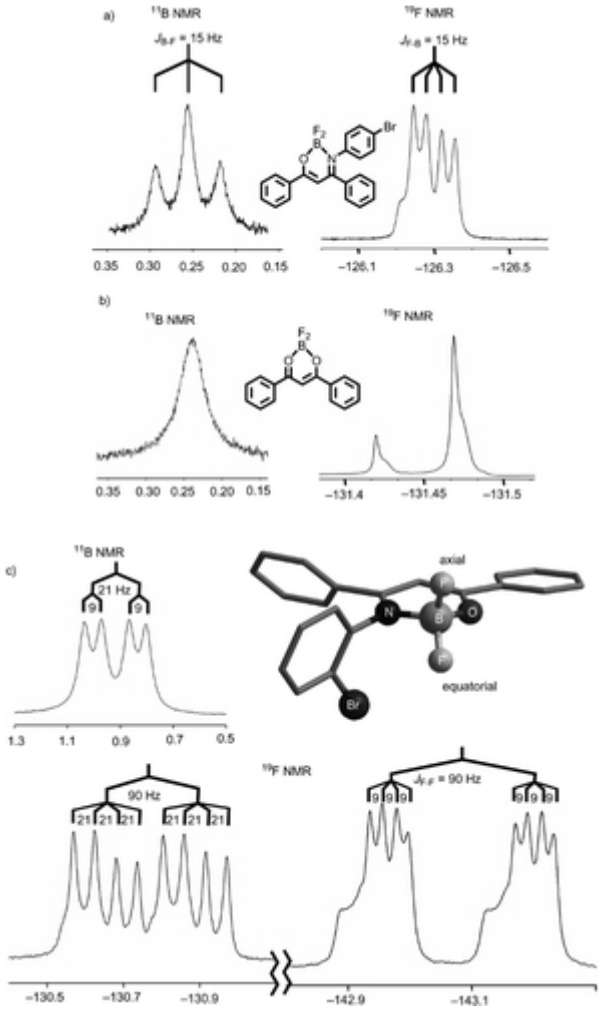

Figure 4. Representative ^{11}B and of ^{19}F NMR spectra obtained for $CDCl_3$ solutions of C_{2v} symmetric BF_2(Ph, H, Ph) (top) and C_1 symmetric BF_2(Ph, H, Ph^{2BrPh}).

Theoretical Studies

In order to facilitate the discussion of the electronic properties of the difluoroboron chelate complexes it is instructive to examine the results obtained from time-dependent density functional calculations (B3LYP/6-31G*, using PM3 energy-minimized structures), which represented a reasonable compromise between computational speed and structural accuracy (see Supporting Information for a comparison of results derived from different basis sets). Regardless of the basis set, the computational results qualitatively agreed with those of previous calculations for related diketonate complexes**8** and the experimental structural trends in electronic data reported here. Figure **5** provides frontier orbitals obtained from single-point energy calculations for thePM3-energy-minimized structures of the three chelates BF_2(*t*Bu,H,*t*Bu), BF_2(*t*Bu,H,tBu^{Ph}), and BF_2(*t*Bu^{Ph},H,tBu^{Ph}).

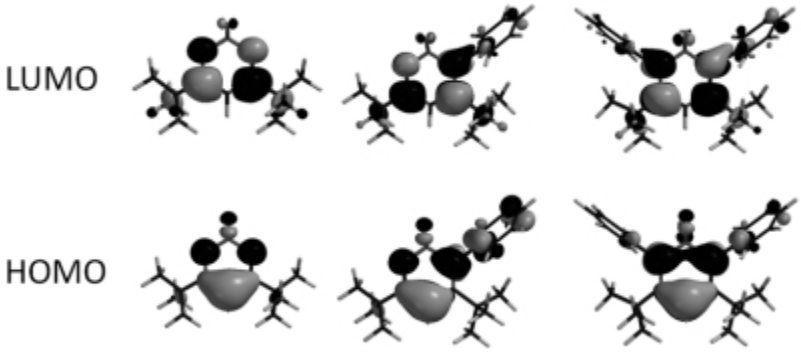

Figure 5. Frontier orbitals for BF_2(*t*Bu, H, *t*Bu) (left), BF_2(*t*Bu, H, *t*Bu^{Ph}) (middle), BF_2(*t*Bu^{Ph}, H, *t*Bu^{Ph}) (right) from DFT (B3LYP/6-31G*) calculations.

These frontier orbitals are representative for the remaining series of diketonate, ketoiminate, and diiminate chelates in that the HOMO and LUMO are mainly centered on the chelate rings. Figure 6 provides a summary of the relative HOMO and LUMO energies of a series of fifteen compounds with varying substitution patterns of heteroatom and chelate ring substituents, from which, a number of features can be extracted. First, the HOMO and LUMO energies increase along the series: β-diketonate < β-ketoiminate < β-diiminate, presumably due to the greater electron-donating nature of (aniline's) nitrogen compared to oxygen. Also apparent from Figure 6 is that the electronic properties of the diketonates are more tuneable than those of the corresponding ketoiminates, which are, in turn, more tuneable than those of diiminates. That is, the variation in the HOMO and LUMO energies with substitution along the chelate ring backbone is greatest for the diketonates and smallest for the diiminates. For chelate rings with only aliphatic substituents on the carbon backbone, the energy of the HOMO varies more than the LUMO on increasing aniline substitution whereas the reverse is true for derivatives with any aryl groups on the chelate ring backbone; the energy of the LUMO varies more than that of the HOMO. Coarse-tuning of the HOMO–LUMO energy gap of the chelates is best achieved by changing the degree of conjugation across the carbon backbone of the chelate rings. As noted previously,[8] replacing aliphatic groups on the carbon backbone of the chelate ring with aromatic groups is sufficient to substantially lower the HOMO–LUMO energy gap (predominantly by changing the LUMO energy) in the β-diketonate series. The increase in HOMO–LUMO energy gap on traversing between BF_2(Ph,H,Ph) (ΔE = 3.97 eV) and BF_2(Ph,Ph,Ph) (ΔE = 4.17 eV) is presumably due to steric interactions that reduce the extent of conjugation in the latter (by lowering the probability of coplanar arrangement of phenyl and chelate rings). Similar arguments explain the trends calculated (and found) for the energy gaps in keto(aryl)iminates and bis(aryl)iminate derivatives with aryl groups decorating both the chelate ring carbon and the nitrogen atoms. Finally, the electronic impact of changing substitution on the aniline groups is calculated to be minimal owing to the negligible contribution of aniline group substituents to either the HOMO or LUMO.

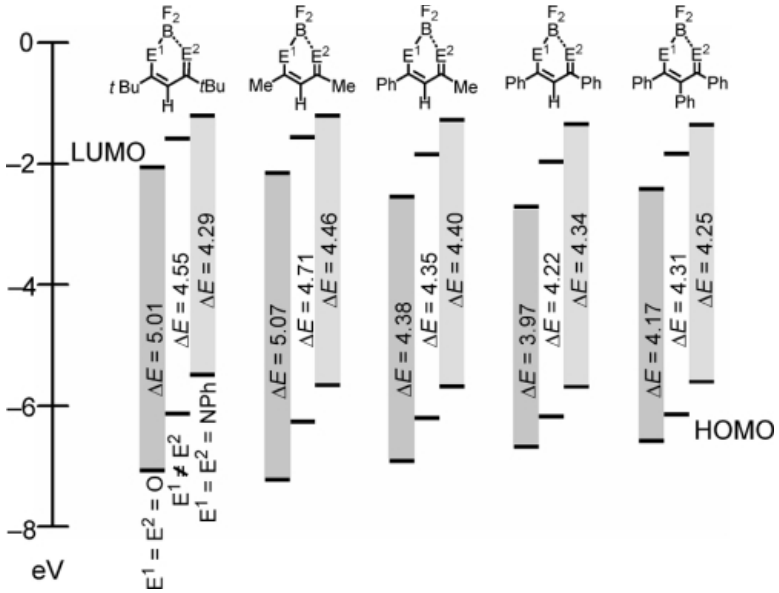

Figure 6. Effect of methyl and phenyl substitution on the relative energies of frontier orbitals for various chelate complexes [obtained from DFT (B3LYP/6-31G*) calculations].

Electronic Properties

A summary of the electronic properties of the difluoroboron complexes prepared in this study is given in Table **3**. The observed properties mirrored those anticipated from the calculations, and those observed for the diketonate series are in agreement with earlier findings. That is, the chelates are all weak electron-acceptors whose properties can be fine-tuned by varying substituents along the periphery. The replacement of electronegative oxygen atom with the more electron-donating aniline substituent renders the chelate a poorer acceptor, as shown for the *tert*-butyl compounds in Figure **7**.

Table 3. Electronic properties of difluoroboron chelate complexes.

Compound	$E_{1/2}$		Absorbance[b]			Emission[b]	Calculated lowest-energy excitation			
	(V vs. Ag/AgCl)[a]									
	(oxid.)	(red.)	λ_{max} (ϵ, M^{-1} cm^{-1})			λ_{max}	λ [eV]	λ [nm]	f[c]	Assignment [eV]
β-Diketonates										
BF_2(*t*Bu,H,*t*Bu)	n.o.[d]	–1.46	221(1424)	291 (23980)		377	5.00	248	0.059	HOMO (–7.07)→LUMO (–2.06)
BF_2(Me,H,Me)	n.o.	–1.40	228 (6440)	286 (16703)		315	5.19	239	0.298	HOMO (–7.22)→LUMO (–2.16)
BF_2(Ph,H,Me)	n.o.	–1.12		261 (3941)	329 (27231)	371	4.32	287	0.328	HOMO (–6.92)→LUMO (–2.55)
BF_2(Ph,H,Ph)	n.o.	–1.93; –0.82		269 (9147)	366 (47210)	414	3.83	324	0.956	HOMO (–6.89)→LUMO (–2.72)
BF_2(Ph,Ph,Ph)	n.o.	–0.83	273 (9193)	314 (10345)	376 (20904)	523	3.59	345	0.173	HOMO (–6.59)→LUMO (–2.44)
BF_2(*p*Anis,H,*p*Anis)	1.98	–2.18, –1.06	251 (6695)	320 (8296)	410 (56767)	443	3.56	348	1.000	HOMO (–6.12)→LUMO (–2.37)
β-Ketoiminates										
BF_2(*t*Bu,H,*t*Bu^{Ph})	2.10	–1.73	214 (4758)		305 (24742)	403	4.29	289	0.260	HOMO (–6.14)→LUMO (–1.59)

BF_2(Me,H,Me^{4BrPh})	2.14	–1.70, –1.81	219 (8626)	301 (12705)		331	4.29	289	0.168	HOMO (–6.38)→LUMO (–1.73)
BF_2(Ph,H,Me^{4BrPh})	2.05	–1.42, –2.22	225 (6394)	253 (4507)	342 (23917)	436, 471, 387[s] [e]	4.02	309	0.431	HOMO (–6.32)→LUMO (–2.00)
BF_2(Ph,H,Ph^{Ph})	2.00	–1.20, –1.88		265 (8729)	360 (22552)	405, 419, 440, 469[s]	3.95	314	0.455	HOMO (–6.18)→LUMO (–1.97)
BF_2(Ph,H,Ph^{2BrPh})	2.16	–1.16, –1.88		264 (8998)	360 (35593)	432, 408, 469[s]	3.86	321	0.083	HOMO (–6.31)→LUMO (–2.09)
BF_2(Ph,H,Ph^{4BrPh})	2.00	–1.15, –1.83	232 (8513)	258 (5588)	362 (25961)	490, 472, 513, 524[s]	3.81	325	0.350	HOMO (–6.27)→LUMO (–2.10)
BF_2(Ph,H,$Ph^{2Br4Tolyl}$)	2.10	–1.19, –1.91		265 (7515)	360 (33121)	418, 407[s]	3.78	328	0.078	HOMO (–6.26)→LUMO (–2.05)
BF_2(Ph,H,Ph^{4pzPh})	1.71	–1.31, –1.80		264 (18664)	366 (27348)	411, 427, 473, 491[s]	3.50	354	0.233	HOMO (–5.99)→LUMO (–2.03)
BF_2(Ph,H,$Ph^{2pz4Tolyl}$)	1.90	–1.20, –1.92	230 (25717)	256 (23367)	362 (25569)	419	3.86	322	0.028	HOMO (–6.11)→LUMO (–1.81)
BF_2(Ph,Ph,Ph^{4BrPh})	1.95	–1.22, –1.76	226 (16168)	249 (10769)	356 (25700)	474	3.89	319	0.096	HOMO (–6.24)→LUMO (–1.97)

BF_2(*p*Anis,H, *p*Anis^{4BrPh})	1.76	–1.24, –1.99	236 (21251)		381 (45764)	449	3.65	340	0.264	HOMO (–5.90)→LUMO (–2.01)
β-Diiminates										
BF_2(Me^{4BrPh},H,Me^{4BrPh})	1.56	–2.09	218 (9860)	246 (4374)	334 (32565)	419	4.30	288	0.568	HOMO (–5.94)→LUMO (–1.49)
BF_2(*t*Bu^{Ph},H,*t*Bu^{Ph})	1.52	–1.83	231 (7647)	264 (2844)	343 (38530)	365	4.18	296	0.597	HOMO (–5.50)→LUMO (–1.21)
BF_2(Ph^{4BrPh},H,Me^{4BrPh})	1.59	–1.59, –2.04	249 (6913)	282 (6186)	353 (27384)	440, 470, 399^{s}	4.18	297	0.428	HOMO (–5.94)→LUMO (–1.56)

[a] CH_3CN, $(NBu_4)(PF_6)$ supporting electrolyte, 100 mV/s scan rate.
[b] CH_3CN, 298 K.
[c] Oscillator strength.
[d] n.o. = not observed.
[e] s: solid-state emission, (298 K).

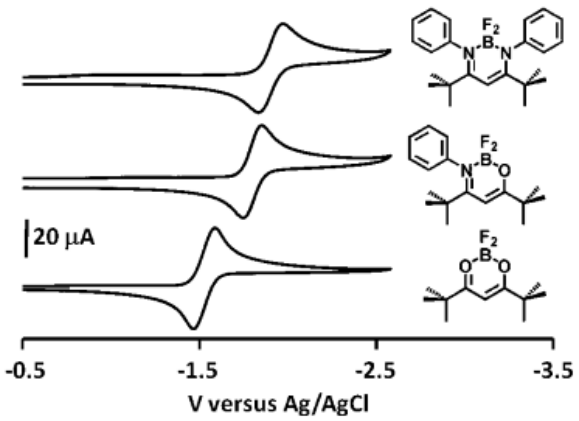

Figure 7.Cyclic voltammograms for CH_3CN solutions of $BF_2(t\text{Bu}^{Ph},H,t\text{Bu}^{Ph})$ (top), $BF_2(t\text{Bu},H,t\text{Bu}^{Ph})$ (middle), and of $BF_2(t\text{Bu},H,t\text{Bu})$ (bottom) obtained at a scan rate of 100 mV/s with $(NBu_4)(PF_6)$ as supporting electrolyte.

In this series, the diketonate exhibits a reversible reduction at –1.6 V (vs. Ag/AgCl), while the ketoiminate and diiminate reductions occur at –1.8 V and –1.9 V, respectively. It should be noted that of the compounds reported here, the reversible nature (i_a/i_c = 1) of the reduction waves is unique to the *tert*-butyl derivatives; the remainder of the chelates exhibit irreversible waves characteristic of EC behavior where the anticipated anodic portion of the wave is either absent or notably less intense than expected. Regardless, the trend holds that the diketonates are easiest and the diiminate the most difficult to (irreversibly) reduce. Within a given series of chelate, the acceptor strength increases with the chelate substituent's capacity for extending π-conjugation, as observed elsewhere for the diketonates.[8] For instance, for the ketoiminates derived from 4-bromoaniline, the reduction becomes more favorable along the series $BF_2(Me,H,Me^{4BrPh})$ (–1.8 V), $BF_2(Ph,H,Me^{4BrPh})$ (–1.4 V), $BF_2(Ph,H,Ph^{4BrPh})$ (–1.2 V), as anticipated for lowering the energy of the LUMO as a result of increased conjugation. Also, of interest is that an anodic wave for an irreversible oxidation is found for each diiminate near 1.6 V while for each ketoiminate the wave is found near the acetonitrile solvent window at about 2.1 V. Presumably, the oxidation for each diketonate occurs outside the potential window, due to the electron-poor nature of the chelate.

The steady-state absorption spectroscopic data of the chelates parallels the results from theoretical TD-DFT calculations (collected in Table 3), which show that the HOMO–LUMO energy gap (approximated by the onset of the lowest energy absorption band) is most effectively coarse-tuned by extending conjugation of the chelate ring. Figure 8 displays the red-shift in the lowest energy absorption band for the ketoiminate series, $BF_2(Me,H,Me^{4BrPh})$, $BF_2(Ph,H,Me^{4BrPh})$, $BF_2(Ph,H,Ph^{4BrPh})$ that typifies the effect of replacing chelate-ring alkyls with phenyl groups in any of the chelate series. Substitution of oxygen for an electron-donating aniline group allows for fine-tuning of the absorption spectrum, since the HOMO and LUMO energies are destabilized by approximately the same extent, as discussed above. Thus, within a series of chelates derived from the same diketonate, there is only a slight blue-shift in the absorption (or emission) spectra with increasing aniline substitution, if it can be detected. Finally, while difluoroboron diketonates have been reported to be fluorescent in the solid state and solution, reports on the luminescent behavior of ketoiminate and diminate derivatives are scarce. All the nitrogenous chelate derivatives reported here are luminescent in the solid state giving green-blue emission but are only very weakly emissive in fluid solution at room temperature, if

emission can be detected at all (Figure 9). The similarity between the spectra of these chelates and those of the diketonates suggests that the emission is fluorescent in nature.

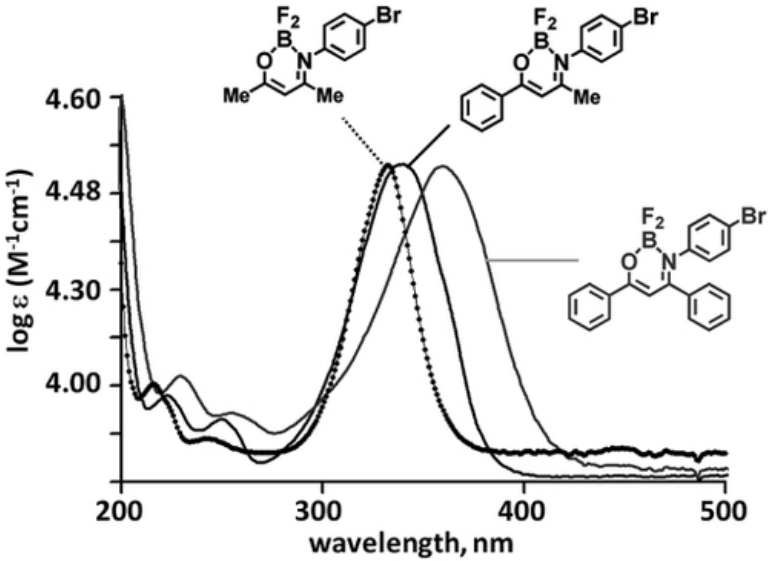

Figure 8. Absorption spectra for ketoimine derivatives of 4-bromoaniline, emphasizing the coarse-tuning of HOMO–LUMO energy gap by substitution of groups capable of extending π-conjugation.

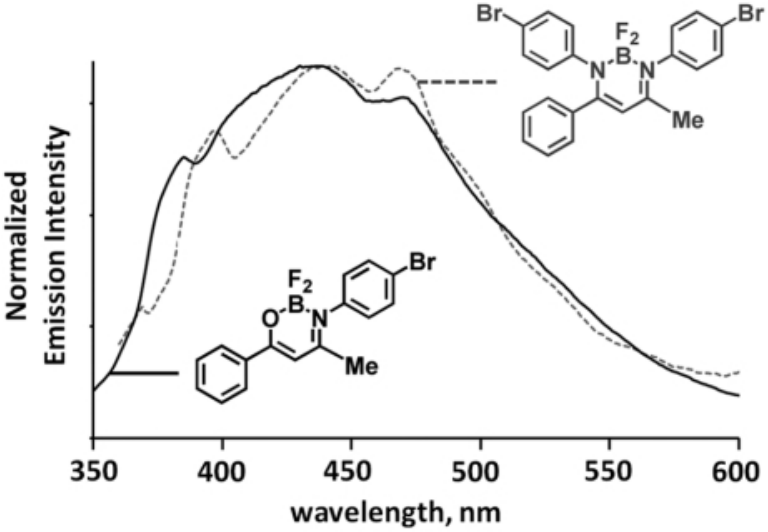

Figure 9. Normalized solid-state emission spectra for representative ketoiminate and diiminate of difluoroboron.

Conclusions

A series of twenty difluoroboron chelates of β-diketonate, β-ketoiminate, and β-diiminates have been prepared and the relationship between structural substitutions and their effect on electronic properties was examined both experimentally and by density functional calculations. The substitution of electron-withdrawing oxygen for more electron-donating aniline groups renders the electroactive boron-based luminophores poorer acceptors and generally results in lower-energy absorption/emission processes. The dominant factor in the tunability of HOMO–LUMO energy gap is the extent of conjugation along the chelate ring backbone. Steric interactions between adjacent aryl substitutents appear to disrupt this conjugation. Electrochemical studies verify that none of the chelate ligands are innocent spectators, as they are all weak electron acceptors where their potency is

maximized for the derivatives of dibenzolymethane. Also, of those compounds studied only the *tert*-butyl derivatives show reversible redox behavior, presumably steric interactions prevent intermolecular decomposition pathways. Thus, proper consideration of the electronic properties and steric demands of these chelating ligands should allow the realization of new examples of low oxidation state transition-metal complexes by our group.

Experimental Section

General Considerations: Solvents were dried and distilled prior to use except where indicated otherwise. Literature procedures were used to prepare H(pzAn^{Me}),[25] the diketone H(Ph,Ph,Ph),[12]the β-ketoimines H(*t*Bu,H,*t*Bu^{Ph}),[13] H(Me,H,Me^{4BrPh}),[26] H(Ph,H,Me^{4BrPh}),[27] H(Ph,H,Ph^{Ph}),[28] H(Ph,H,Ph^{2BrPh}),[29] H(Ph,H,Ph^{4BrPh}),[30] and the β-diimine H(*t*Bu^{Ph},H,*t*Bu^{Ph}).[14] Most of the difluoroboron diketonate derivatives have been reported previously[4,9,15–21] and a summary of the characterization data for the known ligands and complexes can be found in the Supporting Information; the exception is BF_2(Ph,Ph,Ph) described below. All other β-diketones and chemicals were obtained commercially and were used as received. Elemental Analysis was performed by Midwest Microlab Inc., Indianapolis, IN. Melting point determinations were made on samples contained in glass capillaries using an Electrothermal 9100 apparatus and are uncorrected. ^{1}H and ^{13}C NMR spectra were recorded with a Varian 300 MHz spectrometer. Chemical shifts were referenced to solvent resonances at: δ_H = 7.27, δ_C = 77.23 ppm for $CDCl_3$. The ^{11}B (samples in quartz tubes) and ^{19}F NMR spectra were recorded with a Varian 400 MHz spectrometer and were referenced to external samples of $BF_3{\cdot}OEt_2$ and CF_3CO_2H (δ = 0.00 ppm). Absorption measurements were recorded with an Agilent 8453 spectrometer. Steady-state emission spectra were obtained with a JASCO FP-6500 spectrofluorometer. Electrochemical measurements were collected with a BAS CV-50V instrument for ca. 0.2 mM CH_3CN solutions of the complexes, with 0.25 M NBu_4PF_6 as the supporting electrolyte, in a three-electrode cell comprised of a Ag/AgCl electrode, a platinum working electrode and a glassy-carbon counter electrode.

Ketoiminines

H(Ph,Ph,Ph^{4BrPh}): A mixture of 0.63 g (2.1 mmol) H(Ph,Ph,Ph), 0.43 g (2.5 mmol) 4-bromoaniline and *p*-toluenesulfonic acid (about 2 mol-%) in 30 mL of toluene was heated at reflux in a Dean–Stark apparatus for 16 h. Solvent was removed by vacuum distillation and the solid residue was washed with methanol, filtered, and dried under vacuum to leave 0.51 g (54 % yield) H(Ph,Ph,Ph^{4BrPh}) as a yellow solid; m.p. 164.5–165.0 °C. $C_{27}H_{20}BrNO$ (454.37): calcd. C 71.37, H 4.44, N 3.08; found C 71.02, H 4.43, N 2.97. ^{1}H NMR (300 MHz, $CDCl_3$, 22 °C): δ = 7.43–7.37 (m, 2 H), 7.36–7.29 (m, 2 H), 7.23–7.15 (m, 2 H), 7.10–6.97 (m, 8 H), 6.87 (m, 1 H), 6.84 (m, 1 H), 6.82 (d, 2 H), 6.79 (m, 1 H) ppm. ^{13}C NMR (75 MHz, $CDCl_3$, 22 °C): δ = 195.1, 161.5, 142.4, 138.8, 138.7, 134.0, 133.6, 131.8, 129.8, 129.1, 128.7, 128.3, 128.2, 127.5, 127.4, 125.7, 125.2, 117.5, 112.3 ppm. UV/Vis (CH_3CN): λ_{max} (log ϵ) = 379 nm (4.41).

H(Ph,H,Ph^{4pzPh}): A mixture of 1.2 g (3.1 mmol) H(Ph,H,Ph^{4BrPh}), 0.23 g (3.4 mmol) pyrazole, 0.79 g (0.57 mmol) K_2CO_3, 0.07 mL (about. 20 mol-%) DMEDA, and 0.030 g (about 5 mol-%) CuI in 4 mL of xylenes was heated at reflux for 72 h. The product mixture was then washed with deionized water, extracted with dichloromethane and separated. The collected organic phases were dried with magnesium sulfate, filtered, and the solvent was removed in vacuo. Column chromatography (silica gel) using 2:1 hexanes/ethyl acetate (R_f = 0.52) afforded 0.85 g (72 % yield) of H(Ph,H,Ph^{4pzPh}) as a yellow solid;

m.p.130–131 °C. $C_{24}H_{19}N_3O$ (365.43): calcd. C 78.88, H 5.24, N 11.50; found C 79.02, H 5.55, N 11.14. ^{1}H NMR (300 MHz, $CDCl_3$, 22 °C): δ = 12.96 (br. s, 1 H, N/O-H), 7.99 (d, *J* = 6.7 Hz, 2 H, arom.), 7.83 (d, *J* = 3 Hz, 1 H, pz-H_5), 7.68 (d, *J* = 2 Hz, 1 H, pz-H_3), 7.53–7.33 (m, 10 H), 6.88 (d, *J* = 8.9 Hz, 2 H, arom), 6.44 (dd, *J* = 3, 2 Hz, 1 H, pz-H_4), 6.14 [s, 1 H, -C(O)C*H*C(N)-] ppm. ^{13}C NMR (75 MHz, $CDCl_3$, 22 °C): δ = 190.0, 161.4, 141.2, 139.9, 138.0, 136.6, 135.7, 131.6, 130.1, 128.9, 128.6, 128.55, 127.5, 126.8, 124.1, 119.7, 107.8, 97.5 ppm. UV/Vis (nm, CH_3CN): λ_{max} (log ϵ) = 382 (4.45), 274 (4.34).

H(Ph,H,Ph^{2Br4Tolyl}): A mixture of dibenzoylmethane (2.7 g, 12 mmol), 2-bromotoluidine (2.7 g, 14 mmol) and (about 2 mol-%) *p*-toluenesulfonic acid in 30 mL of toluene was heated at reflux for 18 h, and the solvent removed in vacuo. Column chromatography (silica gel, 5:1 hexane/ethyl acetate, R_f = 0.5) followed by recrystallization by cooling a refluxing hexanes solution to room temperature afforded 2.6 g (63 % yield) of H(Ph,H,Ph^{2Br4Tolyl}) as a yellow solid; m.p. 113–114 °C. $C_{22}H_{18}BrNO$ (392.29): calcd. C 67.36, H 4.62, N 3.57; found C 67.20, H 4.76, N 3.80. ^{1}H NMR (300 MHz, $CDCl_3$, 22 °C): δ = 12.73 (br. s, 1 H, N/O-H), 8.00 (d, *J* = 7.3 Hz, 2 H, arom.), 7.52–7.41 (m, 3 H, arom.), 7.40–7.30 (m, 6 H, arom.), 6.70 (part of AB, *J* = 8.1 Hz, 1 H, arom.), 6.37 (part of AB, *J* = 8.2 Hz, 1 H, arom.), 6.17 [s, 1 H, -C(O)C*H*C(N)-], 2.21 (s, 3 H, CH_3) ppm. ^{13}C NMR (75 MHz, $CDCl_3$, 22 °C): δ = 190.2, 161.2, 139.9, 136.1, 136.0, 135.7, 133.4, 131.7, 130.0, 128.8, 128.6, 128.5, 128.2, 127.7, 125.8, 117.6, 98.0, 20.7 ppm. UV/Vis (CH_3CN): λ_{max} (log ϵ) = 376 (4.30), 257 nm (4.20).

H(Ph,H,Ph^{2pz4Tolyl}): A mixture of dibenzoylmethane (3.0 g, 14 mmol), 4-methyl-2-pyrazoylaniline (2.4 g, 14 mmol) and *p*-toluenesulfonic acid (about 2-mol-%) in 30 mL of toluene was heated at reflux for 16 h and the solvent removed in vacuo. Column chromatography (silica gel, 3:1 hexanes/ethyl acetate, R_f = 0.6)followed by recrystallization by cooling a refluxing hexanes solution to room temperature afforded 4.4 g (85 % yield) of H(Ph,H,Ph^{2pz4Tolyl}) as a yellow solid; m.p. 50 °C (glass). $C_{25}H_{21}N_3O$ (379.46): calcd. C 79.13, H 5.58, N 11.07; found C 79.44, H 5.87, N 10.69. ^{1}H NMR (300 MHz, $CDCl_3$, 22 °C): δ = 12.70 (br. s, 1 H, N/O-H), 7.96 (m, 2 H, arom.), 7.84 (d, *J* = 2.3 Hz, 1 H, pz-H_5), 7.76 (d, *J* = 1.7 Hz, 1 H, pz-H_3), 7.54–7.38 (m, 2 H, arom.), 7.38–7.09 (m, 7 H, arom.), 6.88 (part of AB, *J* = 8.2 Hz, 1 H, aniline), 6.73 (part of AB, *J* = 8.2 Hz, 1 H, aniline), 6.48 (dd, *J* = 2.3, 1.7 Hz, 1 H, pz-H_4), 6.08 [s, 1 H, -C(O)C*H*C(N)-], 2.30 (s, 3 H, CH_3) ppm. ^{13}C NMR (75 MHz, $CDCl_3$, 22 °C): δ = 190.0, 161.80, 161.78, 141.14, 140.07, 135.8, 135.6, 131.5, 131.0, 130.4, 129.8, 128.51, 128.50, 128.47, 128.3, 127.5, 127.0, 126.5, 107.4, 97.7, 20.9 ppm. UV/Vis (nm, CH_3CN): λ_{max} (log ϵ) = 382 (4.20).

H(*p*Anis,H,*p*Anis^{4BrPh}): A mixture of 4-bromoaniline (0.13 g, 0.77 mmol), H(*p*Anis,H,*p*Anis) (0.22 g, 0.77 mmol) and *p*TsOH (3.1 mg, 0.015 mmol, 2 mol-%) in 80 mL of toluene was heated at reflux overnight with a Dean–Stark trap to remove water. The solvent was removed by rotary evaporation and the crude product was purified on a silica gel column using ethyl acetate/hexane (1:5) as the eluent to give the product in a yellow band (R_f = 0.37). After removing solvent under vacuum and recrystallization by cooling a hot saturated hexanes solution to –20 °C, 0.16 g (47 %) of H(*p*Anis,H,*p*Anis^{BrPh}) was obtained as yellow needles; m.p. 62–64 °C. $C_{23}H_{12}BrNO_3$ (430.26): calcd. C 64.21, H 2.81, N 3.26, found C 64.03, H 3.02, N 3.33. ^{1}H NMR (300 MHz, $CDCl_3$, 22 °C): δ = 12.70 (br. s, 1 H, N/O-H), 7.95 (d, *J* = 9.1 Hz, 2 H), 7.33 (d, *J* = 8.9 Hz, 2 H), 7.24 (d, *J* = 8.9 Hz, 2 H), 6.95 (d, *J* = 8.9 Hz, 2 H), 6.87 (d, *J* = 9.1 Hz, 2 H), 6.66 (d, *J* = 8.9 Hz, 2 H), 6.06 [s, 1 H,-C(O)C*H*C(N)-], 3.87 (s, 3 H, -OCH_3), 3.84 (s, 3 H, -OCH_3) ppm. ^{13}C NMR (75 MHz, $CDCl_3$, 22 °C): δ = 189.0, 162.6, 161.1, 160.3, 139.4, 132.7, 131.9, 130.1, 129.5, 127.9, 124.6,

116.8, 114.3, 113.8, 97.2, 55.6, 55.5 ppm. UV/Vis (CH_2Cl_2): λ_{max} (log ϵ) = 389 (4.62), 287 (4.48), 229 nm (4.53).

Diimines

H(Me^{4BrPh},H,Me^{4BrPh}): A mixture of 4-bromoaniline (3.61 g, 21.0 mmol), acetylacetone (1.00 g, 9.99 mmol) and *p*TsOH (0.0039 g, 0.20 mmol, 2 mol-%) in 80 mL of toluene was heated at reflux overnight with a Dean–Stark trap to remove water. The solvent was removed by rotary evaporation and the crude product was purified on a silica gel column using acetone/hexane (1:4) to give the product in the first yellow band (R_f = 0.53). A sample of pure H(Me^{BrPh},H,Me^{BrPh}) (1.14 g, 28 %) was obtained as yellow needles after recrystallization from hexane at –20 °C; m.p. 107–108 °C. $C_{17}H_{16}Br_2N_2$ (408.13): calcd. C 50.03, H 3.95, N 6.86; found C 50.34, H 3.97, N 7.13. ^{1}H NMR (300 MHz, $CDCl_3$, 22 °C): δ = 12.60 (br. s, 1 H, NH), 7.39 (part of AA'BB', *J* = 8.6 Hz, 4 H, aniline), 6.82 (part of AA'BB', *J* = 8.6 Hz, 4 H, aniline), 4.89 [s, 1 H, -C(N)C*H*C(N)-], 1.98 (s, 3 H, -CH_3) ppm. ^{13}C NMR (75 MHz, $CDCl_3$, 22 °C): δ = 159.8, 144.8, 132.0, 124.3, 116.4, 98.2, 21.0 ppm. UV/Vis (CH_2Cl_2): λ_{max} (log ϵ) = 349 (4.56), 233 nm (4.52). A sample of H(Me,H,Me^{BrPh}) (1.05 g, 4.13 mmol, 41 %, based on acetylacetone) as pale yellow needles was obtained after eluting a second yellow band (R_f = 0.42) from the column and after recrystallization from hexane at –20 °C, to afford the known ketoiminate as yellowish crystals; m.p. 53–55 °C. ^{1}H NMR (300 MHz, $CDCl_3$, 22 °C): δ = 12.60 (br. s, 1 H, N/O-H), 7.39 (d, *J* = 8.6 Hz, 4 H), 6.82 (d, *J* = 8.6 Hz, 4 H), 4.89 [s, 1 H, -C(O)C*H*C(N)-], 1.98 (s, 3 H, -CH_3) ppm. ^{13}C NMR (75 MHz, $CDCl_3$, 22 °C): δ = 196.7, 159.7, 138.1, 132.3, 126.3, 118.8, 98.4, 29.4, 20.0 ppm. UV/Vis (CH_2Cl_2): λ_{max} (log ϵ) = 330 (4.41), 229 (4.19).

H(Ph^{4BrPh},H,Me^{4BrPh}): A mixture of 4-bromoaniline (4.50 g, 26.2 mmol), benzoylacetone (2.02 g, 12.5 mmol) and *p*TsOH (4.9 mg, 0.25 mmol, 2 mol-%) in 80 mL of toluene was heated at reflux overnight with a Dean–Stark trap to remove water. After removing solvent by rotary evaporation the crude product mixture was subject to column chromatography on silica gel using 1:4 acetone/hexane as an eluent to give the desired product in the first yellow band (R_f = 0.68). A 0.35 g (10 %) sample of pure H(Ph^{BrPh},H,Me^{BrPh}) was obtained after recrystallization from hexanes at –20 °C; m.p. 163–165 °C. $C_{22}H_{18}Br_2N_2$ (470.21): calcd. C 56.20, H 3.86, N 5.96; found C 56.58, H 4.12, N 5.63. ^{1}H NMR (300 MHz, $CDCl_3$, 22 °C): δ = 12.50 (br. s, 1 H, NH), 7.43 (part of AA'BB', *J* = 8.7 Hz, 2 H, aniline), 7.33 (m, 5 H, phenyl), 7.15 (part of AA'BB', *J* = 8.5 Hz, 2 H, aniline), 6.78 (part of AA'BB', *J* = 8.5 Hz, 2 H, aniline), 6.50 (part of AA'BB', *J* = 8.7 Hz, 2 H, aniline), 5.17 [s, 1 H, -C(N)C*H*C(N)-], 2.00 (s, 3 H, -CH_3) ppm. ^{13}C NMR (75 MHz, $CDCl_3$, 22 °C): δ = 166.2, 154.8, 148.5, 141.4, 137.0, 132.0, 131.7, 129.1, 128.7, 128.4, 123.6, 123.4, 116.4, 115.2, 102.2, 21.7 ppm. UV/Vis (CH_2Cl_2): λ_{max} (log ϵ) = 365 (4.46), 267 (4.37), 230 nm (4.47). The known H(Ph,H,Me^{BrPh}) (1.51 g, 9.31 mmol, 74 %, based on benzoylacetone) was obtained after elution of a second yellow band from the column (R_f = 0.51) and recrystallization from hexanes at –20 °C; m.p. 130–132 °C. ^{1}H NMR (300 MHz, $CDCl_3$, 22 °C): δ = 13.10 (br. s, 1 H, N/O-H), 7.91 (part of AA'BB', *J* = 8.0 Hz, 2 H, aniline), 7.45 (m, 5 H, phenyl), 7.06 (part of AA'BB', *J* = 8.0 Hz, 2 H, aniline), 5.92 [s, 1 H, -C(O)C*H*C(N)-], 2.14 (s, 3 H, -CH_3) ppm. ^{13}C NMR (75 MHz, $CDCl_3$, 22 °C): δ = 189.1, 161.7, 139.9, 137.9, 132.4, 131.2, 128.5, 127.2, 126.3, 119.0, 94.9, 20.5 ppm. UV/Vis (CH_2Cl_2): λ_{max} (log ϵ) = 361 (4.50), 250 (4.30), 229 nm (4.32).

Difluoroboron Diketonates

BF_2(Ph,Ph,Ph): A mixture of H(Ph,Ph,Ph) (1.0 g, 3.4 mmol) and BF_3·Et_2O (0.48 g, 3.4 mmol) in 15 mL of toluene was heated at reflux for 12 h. After removing the solvent by vacuum distillation and washing

the insoluble solid with dichloromethane, 1.10 g (95 % yield) of BF_2(Ph,Ph,Ph) was obtained as a yellow-green solid; m.p. 315–317 °C. $C_{21}H_{19}BF_2O_2$ (348.16): calcd. C 72.45, H 4.34; found C 72.78, H 4.63. ^{1}H NMR (300 MHz, $CDCl_3$, 22 °C): δ = 7.48–7.37 (m, 6 H, Ph), 7.34–7.21 (m, 7 H, Ph), 7.06 (dd, 2 H, Ph) ppm. ^{13}C NMR (75 MHz, $CDCl_3$, 22 °C): δ = 189.2, 137.4, 137.2, 137.0, 136.0, 134.2, 133.1, 132.5, 132.0, 78.0 ppm. ^{11}B NMR (128 MHz, $CDCl_3$, 22 °C): δ = 0.52 (s, $\omega_{1/2}$ = 19 Hz) ppm. ^{19}F NMR (376 MHz, $CDCl_3$, 22 °C): δ = –138.5 ppm. UV/Vis (CH_2Cl_2): λ_{max} (log ϵ) = 376 (4.32), 314 (3.92), 273 nm (3.96). Other characterization can be found in Table 2 and Table 3.

Difluoroboron Ketoiminates

BF_2(*t*Bu,H,*t*Bu^{Ph}): A mixture of H(*t*Bu,H,*t*Bu^{Ph}) (0.33 g, 0.99 mmol) and BF_3·OEt_2 (0.14 g, 0.99 mmol) afforded 0.23 g (76 % yield) of BF_2(*t*Bu,H,*t*Bu^{Ph}) as a colorless solid; m.p. 167–168 °C. $C_{17}H_{24}BF_2NO$ (307.19): calcd. C 66.47, H 7.87, N 4.56; found C 66.53, H 7.99, N 4.25. ^{1}H NMR (300 MHz, $CDCl_3$, 22 °C): δ = 7.44–7.20 (m, 5 H, phenyl), 5.87 [s, 1 H, -C(O)C*H*C(N)-], 1.29 [s, 9 H, (C*H*$_3$)$_3$CC(O)], 1.12 [s, 9 H, (C*H*$_3$)$_3$CC(N)] ppm. ^{13}C NMR (75 MHz, $CDCl_3$, 22 °C): δ = 180.8, 167.9, 141.1, 128.4, 128.1, 128.0, 92.3, 31.1, 27.9 ppm. ^{11}B NMR (128 MHz, $CDCl_3$, 22 °C): δ = 0.60 (t, $J_{B–F}$ = 14.9 Hz) ppm. ^{19}F NMR (376 MHz, $CDCl_3$, 22 °C): δ = –137.5 (q, J_{B-F} = 14.9 Hz) ppm. Other characterization can be found in Table 2 and Table 3. Crystals suitable for single-crystal X-ray diffraction were grown by slow cooling of a hexanes solution.

BF_2(Me,H,Me^{4BrPh}): A mixture of H(Me,H,Me^{4BrPh}) (0.11 g, 0.43 mmol) and BF_3·OEt_2 (0.060 g, 0.43 mmol) afforded 0.090 g (67 % yield) of BF_2(Me,H,Me^{4BrPh}) as a colorless solid; m.p. 144–145 °C. $C_{11}H_{11}N_1O_2BBrF_2$ (301.93): calcd. C 43.76, H 3.67, N 4.64; found C 44.08, H 3.67, N 4.72. ^{1}H NMR (300 MHz, $CDCl_3$, 22 °C): δ = 7.57 (part of AA'BB', *J* = 8.5 Hz, 2 H, arom.), 7.10 (part of AA'BB', *J* = 8.5 Hz, 2 H, arom.), 5.56 [s, 1 H, -C(O)C*H*C(N)-], 2.20 [s, 3 H, -C(O)C*H*$_3$],1.96 [s, 3 H, -C(N)C*H*$_3$] ppm. ^{13}C NMR (75 MHz, $CDCl_3$, 22 °C): δ = 171.7, 138.9, 138.7, 128.2, 122.4, 99.1, 23.1, 21.5 ppm. ^{11}B NMR (128 MHz, $CDCl_3$, 22 °C): δ = 0.31 (t, $J_{B–F}$ = 15.2 Hz) ppm. ^{19}F NMR (376 MHz, $CDCl_3$, 22 °C): δ = –134.5 (q, J_{B-F} = 15.2 Hz) ppm. Other characterization can be found in Table 2 and Table 3. Crystals suitable for single-crystal X-ray diffraction were grown by slow cooling of a methanol solution.

BF_2(Ph,H,Me^{4BrPh}): A mixture of H(Ph,H,Me^{4BrPh}) (0.80 g, 2.5 mmol) and BF_3·OEt_2 (0.36 g, 2.5 mmol) afforded 0.83 g (91 % yield) of BF_2(Ph,H,Me^{4BrPh}) as a colorless solid; m.p. (dec.) >150 °C. $C_{16}H_{13}BBrF_2NO$ (364.00): calcd. C 52.80, H 3.60, N 3.85; found C 52.63, H 3.70, N 3.54. ^{1}H NMR (300 MHz, $CDCl_3$, 22 °C): δ = 8.00 (d, *J* = 7.6, 7.1 Hz, 2 H, *m*-Ph), 7.59 (part of AA'BB', *J* = 8.5 Hz, 2 H, aniline), 7.56 (t, *J* = 7.1 Hz, 1 H, *p*-Ph), 7.48 (t, *J* = 7.6 Hz, 2 H, *o*-Ph), 7.16 (part of AA'BB', *J* = 8.5 Hz, 2 H, aniline), 6.24 [s, 1 H, -C(O)C*H*C(N)-], 2.11 [s, 3 H, -C(N)C*H*$_3$] ppm. ^{13}C NMR (75 MHz, $CDCl_3$, 22 °C): δ = 172.0, 139.9, 132.9, 132.8, 128.1, 127.7, 126.3, 122.4, 95.9, 22.1 ppm. ^{11}B NMR (128 MHz, $CDCl_3$, 22 °C): δ = 0.64 (t, J_{B-F} = 14.8 Hz) ppm. ^{19}F NMR (376 MHz, $CDCl_3$, 22 °C): δ = –135.0 (q, J_{B-F} = 14.8 Hz) ppm. Other characterization can be found in Table 2 and Table 3.

BF_2(Ph,H,Ph^{Ph}): A mixture of H(Ph,H,Ph^{Ph}) (1.9 g, 6.5 mmol) and BF_3·OEt_2 (0.93 g, 6.5 mmol) afforded 2.2 g (97 % yield) of BF_2(Ph,H,Ph^{Ph})**9a** as a yellow solid; m.p. 195.0–196.5 °C. $C_{21}H_{16}BF_2NO$ (347.17): calcd. C 72.65, H 4.65, N 4.03; found C 72.27, H 4.86, N 4.29. ^{1}H NMR (300 MHz, $CDCl_3$, 22 °C): δ = 8.05 (m, 2 H, Ph), 7.57 (m, 1 H, Ph), 7.48 (m, 2 H, *m*-Ph), 7.37–7.13 (m, 10 H, Ph), 6.41 [s, 1 H, -C(O)C*H*C(N)-] ppm. ^{13}C NMR (75 MHz, $CDCl_3$, 22 °C): δ = 172.3, 170.8, 140.66, 140.65, 133.0, 130.7, 129.0, 128.9, 128.8, 128.7, 127.9, 127.5, 127.1, 97.0 ppm. ^{11}B NMR (128 MHz, $CDCl_3$, 22 °C): δ = 1.11 (t, J_{B-F} = 15.0 Hz)

ppm. ^{19}F NMR (376 MHz, $CDCl_3$, 22 °C): δ = –134.5 (q, $J_{B\text{-}F}$ = 15.0 Hz) ppm. Other characterization can be found in Table 2 and Table 3. Crystals suitable for single-crystal X-ray diffraction were grown by slow diffusion of a layer of hexanes into a dichloromethane solution.

BF_2(Ph,H,Ph^{2BrPh}): A mixture of H(Ph,H,Ph^{2BrPh}) (0.36 g, 0.95 mmol) and BF_3·OEt_2 (0.14 g, 0.95 mmol) afforded 0.22 g (55 % yield) of BF_2(Ph,H,Ph^{2BrPh}) as a yellow solid; m.p. 203.5–204.0 °C. $C_{21}H_{15}BBrF_2NO$ (426.07): calcd. C 59.20, H 3.55, N 3.29; found C 59.41, H 3.74, N 3.30. ^{1}H NMR (300 MHz, $CDCl_3$, 22 °C): δ = 8.09 (m, 2 H, Ph), 7.65 (m, 1 H, aniline), 7.58 (m, 1 H, aniline), 7.51 (m, 2 H, Ph), 7.46–7.24 (m, 7 H, Ph, aniline), 7.11 (m, 1 H, aniline), 6.46 [s, 1 H, -C(O)C*H*C(N)-] ppm. ^{13}C NMR (75 MHz, $CDCl_3$, 22 °C): δ = 133.6, 133.2, 131.0, 130.0, 129.4, 129.0, 128.96, 128.3, 128.1, 127.9, 121.1, 96.8 ppm. ^{11}B NMR (128 MHz, $CDCl_3$, 22 °C): δ = 0.92 (dd, $J_{B\text{-}F}$ = 21, 8 Hz) ppm. ^{19}F NMR (376 MHz, $CDCl_3$, 22 °C): δ = –129.2 (dq, $J_{F\text{-}F}$ = 90, $J_{B\text{-}F}$ = 21 Hz), –142.2 (dq, $J_{F\text{-}F}$ = 90, $J_{B\text{-}F}$ = 8 Hz) ppm. Other characterization can be found in Table 2 and Table 3. Crystals suitable for single-crystal X-ray diffraction were grown by slow diffusion of a layer of hexanes into a dichloromethane solution.

BF_2(Ph,H,Ph^{4BrPh}): A mixture of H(Ph,H,Ph^{4BrPh}) (0.73 g, 1.9 mmol) and BF_3·OEt_2 (0.27 g, 1.9 mmol) afforded 0.75 g (91 % yield) of BF_2(Ph,H,Ph^{4BrPh}) as a yellow solid; m.p. 256–258 °C. $C_{21}H_{15}BBrF_2NO$ (426.07): calcd. C 59.20, H 3.55, N 3.29; found C 58.87, H 3.59, N 3.22. ^{1}H NMR (300 MHz, $CDCl_3$, 22 °C): δ = 8.06 (m, 2 H, Ph), 7.60 (t, *J* = 7.2 Hz, 1 H, *p*-Ph), 7.50 (m, 2 H, Ph), 7.43–7.23 (m, 8 H, Ph, aniline), 7.05 (part of AA'BB', *J* = 8.6 Hz, 2 H, aniline), 6.43 [s, 1 H, -C(O)C*H*C(N)-] ppm. ^{13}C NMR (75 MHz, $CDCl_3$, 22 °C): δ = 170.9, 139.8, 133.3, 132.1, 131.0, 129.0, 128.9, 128.79, 128.78, 128.77, 128.0, 121.4, 97.2 ppm. ^{11}B NMR (128 MHz, $CDCl_3$, 22 °C): δ = 1.01 (t, $J_{B\text{-}F}$ = 15.0 Hz) ppm. ^{19}F NMR (376 MHz, $CDCl_3$, 22 °C): δ = –134.3 (q, $J_{B\text{-}F}$ = 15.0 Hz) ppm. Other characterization can be found in Table 2 and Table 3. Crystals suitable for single-crystal X-ray diffraction were grown by slow diffusion of a layer of hexanes into a dichloromethane solution.

BF_2(Ph,H,Ph^{2Br4Tolyl}): A mixture of H(Ph,H,Ph^{2Br4Tolyl}) (1.1 g, 2.7 mmol) and BF_3·OEt_2 (0.38 g, 2.7 mmol) afforded 1.0 g (83 % yield) of BF_2(Ph,H,Ph^{2Br4Tolyl}) as a yellow solid; m.p. 215–216 °C. $C_{22}H_{17}BBrF_2NO$ (440.09): calcd. C 60.04, H 3.89, N 3.18; found C 60.00, H 3.77, N 2.99. ^{1}H NMR (300 MHz, $CDCl_3$, 22 °C): δ = 8.08 (m, 2 H, Ph), 7.62–7.55 (m, 1 H, Ph), 7.54–7.46 (m, 3 H, Ph), 7.43–7.34 (m, 3 H, Ph), 7.33–7.25 (m, 2 H, Ph), 7.21 (s, 1 H, aniline), 7.14 (part of AB, *J* = 8.1 Hz, 1 H, aniline), 6.44 [s, 1 H,-C(O)C*H*C(N)-], 2.27 (s, 3 H, CH_3) ppm. ^{13}C NMR (75 MHz, $CDCl_3$, 22 °C): δ = 173.3, 172.3, 139.8, 136.9, 134.9, 134.0, 133.2, 131.0, 129.5, 129.0, 128.7, 128.3, 128.1, 122.4, 120.6, 96.8, 21.0 ppm. ^{11}B NMR (128 MHz, $CDCl_3$, 22 °C): δ = 0.89 (dd, $J_{B\text{-}F}$ = 21, 8 Hz) ppm. ^{19}F NMR (376 MHz, $CDCl_3$, 22 °C): δ = –129.4 (dq, $J_{F\text{-}F}$ = 88, $J_{B\text{-}F}$ = 21 Hz), –142.4 (dq, $J_{F\text{-}F}$ = 88, $J_{B\text{-}F}$ = 8 Hz) ppm. Other characterization can be found in Table 2 and Table 3. Crystals suitable for single-crystal X-ray diffraction were grown by slow diffusion of a layer of hexanes into a dichloromethane solution.

BF_2(Ph,H,Ph^{4pzPh}): A mixture of H(Ph,H,Ph^{4pzPh}) (0.46 g, 1.3 mmol) and BF_3·OEt_2 (0.18 g, 1.3 mmol) afforded 0.45 g (86 % yield) of BF_2(Ph,H,Ph^{4pzPh}) as a yellow solid; m.p. 229–230 °C. $C_{24}H_{18}BF_2N_3O$ (413.23): calcd. C 69.76, H 4.39, N 10.17; found C 69.98, H 4.15, N 10.23. ^{1}H NMR (300 MHz, $CDCl_3$, 22 °C): δ = 8.06 (part of AA'BB', *J* = 8.05 Hz, 2 H, aniline), 7.86 (d, 1 H, pz-H_5), 7.69 (d, 1 H, pz-H_3), 7.63–7.44 (m, 5 H, Ph), 7.40–7.19 (m, 7 H, Ph), 6.46 [s, 1 H, -C(O)C*H*C(N)-], 6.42 (dd, *J* = 2.1 Hz, 1 H, pz-H_4) ppm. ^{13}C NMR (75 MHz, $CDCl_3$, 22 °C): δ = 172.7, 170.9, 141.5, 139.0, 138.8, 134.8, 133.2, 130.9, 129.0, 128.9, 128.8, 127.9, 126.9, 119.3, 108.1, 97.2 ppm. ^{11}B NMR (128 MHz, $CDCl_3$, 22 °C): δ = 1.11 (t, $J_{B\text{–}F}$ =

15.0 Hz) ppm. ^{19}F NMR (376 MHz, $CDCl_3$, 22 °C): δ = –134.4 (q, $J_{B\text{-}F}$ = 15.0 Hz) ppm. Other characterization can be found in Table 2 and Table 3. Crystals suitable for single-crystal X-ray diffraction were grown by slow diffusion of a layer of hexanes into a dichloromethane solution.

BF_2(Ph,H,Ph^{2pz4Tolyl}): A mixture of H(Ph,H,Ph^{2pz4Tolyl}) (2.0 g, 5.4 mmol) and BF_3·OEt_2 (0.76 g, 5.4 mmol) afforded 0.76 g (33 % yield) of BF_2(Ph,H,Ph^{2pz4Tolyl}) as a yellow solid; m.p. 153–155 °C. $C_{25}H_{20}BF_2N_3O$ (427.26): calcd. C 70.28, H 4.72, N 9.83; found C 70.17, H 5.01, N 9.80. ^{1}H NMR (300 MHz, $CDCl_3$, 22 °C): δ = 8.07–8.04 (m, 2 H, Ph), 7.77 (dd, J = 3 Hz, 1 H, pz-H_5), 7.72 (part of AB, J = 8 Hz, 1 H, aniline), 7.60 (s, 1 H, aniline), 7.54–7.48 (m, 2 H, Ph), 7.47 (d, J = 2 Hz, 1 H, pz-H_3), 7.33 (part of AB, J = 8 Hz, 1 H, aniline), 7.29–7.22 (m, 2 H, Ph), 7.16 (m, 2 H, Ph), 6.76 (d, J = 8.3 Hz, 2 H, Ph), 6.32 (dd, J = 3, 2 Hz, 1 H, pz-H_4), 6.24 [s, 1 H, -C(O)C*H*C(N)-], 2.35 (s, 3 H, CH_3) ppm. ^{13}C NMR (75 MHz, $CDCl_3$, 22 °C): δ = 172.7, 172.3, 140.7, 139.6, 135.6, 135.5, 133.3, 131.2, 130.54, 130.45, 130.2, 129.4, 129.1, 129.0, 128.7, 128.6, 128.2, 128.0, 126.7, 107.8, 21.1 ppm. ^{11}B NMR (128 MHz, $CDCl_3$, 22 °C): δ = 1.06 (dd, $J_{B\text{-}F}$ = 20, 9 Hz) ppm. ^{19}F NMR (376 MHz, $CDCl_3$, 22 °C): δ = –127.4 (dq, $J_{F\text{-}F}$ = 90, $J_{B\text{-}F}$ = 20 Hz), –139.7 (dq, $J_{F\text{-}F}$ = 90, $J_{B\text{-}F}$ = 9 Hz) ppm. Other characterization can be found in Table 2 and Table 3. Crystals suitable for single-crystal X-ray diffraction were grown by slow diffusion of a layer of hexanes into a dichloromethane solution.

BF_2(Ph,Ph,Ph^{4BrPh}): A mixture of H(Ph,Ph,Ph^{4BrPh}) (0.31 g, 0.67 mmol) and BF_3·OEt_2 (0.095 g, 0.67 mmol) afforded 0.33 g (97 % yield) of BF_2(Ph,Ph,Ph^{4BrPh}) as a yellow solid; m.p. 205–206 °C. $C_{27}H_{19}BBrF_2NO$ (422.26): calcd. C 64.58, H 3.81, N 2.79; found C 64.62, H 3.97, N 2.96. ^{1}H NMR (300 MHz, $CDCl_3$, 22 °C): δ = 7.43–7.29 (m, 4 H, Ph), 7.23–7.15 (m, 2 H, arom), 7.10- 6.97 (m, 8 H, Ph), 6.85 (part of AA'BB', J = 7.3 Hz, 2 H, aniline), 6.80 (part of AA'BB', J = 7.3 Hz, 2 H, aniline) ppm. ^{13}C NMR (75 MHz, $CDCl_3$, 22 °C): δ = (CN not obsd.), 135.4, 132.8, 131.9, 131.1, 130.1, 129.2, 129.0, 128.7, 128.4, 127.94, 127.90, 127.3, 121.5, 120.8 ppm. ^{11}B NMR (128 MHz, $CDCl_3$, 22 °C): δ = 0.59 (t, $J_{B\text{-}F}$ = 14.1 Hz) ppm. ^{19}F NMR (376 MHz, $CDCl_3$, 22 °C): δ = –133.3 (q, $J_{B\text{-}F}$ = 14.1 Hz) ppm. Other characterization can be found in Table 2 and Table 3. Crystals suitable for single-crystal X-ray diffraction were grown by slow diffusion of a layer of hexanes into a dichloromethane solution.

BF_2(*p*Anis,H,*p*Anis^{4BrPh}): A mixture of H(*p*Anis,H,*p*Anis^{4BrPh}) (0.38 g, 0.87 mmol) and BF_3·OEt_2 (0.12 g, 0.87 mmol) afforded 0.27 g (64 % yield) of BF_2(*p*Anis,H,*p*Anis^{4BrPh}) as a yellow solid; m.p. 173.5–174.5 °C. $C_{23}H_{19}BBrF_2NO$ (486.12): calcd. C 56.83, H 3.94, N 2.88; found C 57.11, H 3.82, N 3.24. ^{1}H NMR (300 MHz, $CDCl_3$, 22 °C): δ = 8.02 (part of AA'BB', J = 9.0 Hz, 2 H, arom.), 7.36 (part of AA'BB', J = 8.7 Hz, 2 H, aniline), 7.20 (part of AA'BB', J = 8.9 Hz, 2 H, arom.), 7.04 (part of AA'BB', J = 8.7 Hz, 2 H, aniline), 6.98 (part of AA'BB', J = 9.0 Hz, 2 H, arom.), 6.80 (part of AA'BB', J = 8.9 Hz, 2 H, arom.), 6.32 [s, 1 H, -C(O)C*H*C(N)-], 3.90 (s, 3 H, OCH_3), 3.81 (s, 3 H, -OCH_3) ppm. ^{13}C NMR (75 MHz, $CDCl_3$, 22 °C): δ = 163.9, 161.6, 132.1, 131.0, 130.1, 128.8, 120.9, 114.4, 114.3, 55.8, 55.6 ppm. ^{11}B NMR (128 MHz, $CDCl_3$, 22 °C): δ = 0.99 (t, $J_{B\text{-}F}$ = 15.5 Hz) ppm. ^{19}F NMR (376 MHz, $CDCl_3$, 22 °C): δ = –135.4 (q, $J_{B\text{-}F}$ = 15.5 Hz) ppm. Other characterization can be found in Table 2 and Table 3. Crystals suitable for single-crystal X-ray diffraction were grown by slow diffusion of a layer of hexanes into a dichloromethane solution.

Difluoroboron Diiminates

BF_2(*t*Bu^{Ph},H,*t*Bu^{Ph}): A mixture of H(*t*Bu^{Ph},H,*t*Bu^{Ph}) (1.9 g, 5.7 mmol) and BF_3·OEt_2 (0.81 g, 5.7 mmol) afforded 1.7 g (79 % yield) of BF_2(*t*Bu^{Ph},H,*t*Bu^{Ph}) as a very pale yellow solid; m.p. 197–201 °C. $C_{23}H_{29}BF_2N_2$ (382.30): calcd. C 72.26, H 7.65, N 7.33; found C 71.98, H 7.93, N 7.47. ^{1}H NMR (300 MHz,

$CDCl_3$, 22 °C): δ = 7.35–7.20 (m, 10 H, Ph), 5.87 [s, 1 H, -C(N)C*H*C(N)-], 1.19 [s, 18 H, -C(CH_3)$_3$] ppm. ^{13}C NMR (75 MHz, $CDCl_3$, 22 °C): δ = 210.0, 173.2, 142.6, 129.3, 128.0, 127.1, 93.6, 31.7 ppm. ^{11}B NMR (128 MHz, $CDCl_3$, 22 °C): δ = 0.92 (t, $J_{B\,F}$ = 29.0 Hz) ppm. NMR (376 MHz, $CDCl_3$, 22 °C): δ = –136.3 (q, $J_{B\text{-}F}$ = 29.0 Hz) ppm. Other characterization can be found in Table 2 and Table 3. Crystals suitable for single-crystal X-ray diffraction were grown by slow cooling of a hexanes solution.

BF_2(Me^{4BrPh},H,Me^{4BrPh}): A mixture of H(Me^{4BrPh},H,Me^{4BrPh}) (0.58 g, 1.4 mmol) and BF_3·OEt_2 (0.20 g, 1.4 mmol) afforded 0.21 g (33 % yield) of BF_2(Me^{4BrPh},H,Me^{4BrPh}) as a colorless solid; m.p. dec. 250 °C. $C_{17}H_{15}BBr_2F_2N_2$ (455.94): calcd. C 44.78, H 3.32, N 6.14; found C 44.92, H 3.01, N 6.07. ^{1}H NMR (300 MHz, $CDCl_3$, 22 °C): δ = 7.52 (part of AA'BB', *J* = 8.6 Hz, 4 H, aniline), 7.12 (part of AA'BB', *J* = 8.6 Hz, 4 H, aniline), 5.25 [s, 1 H, -C(N)C*H*C(N)-], 1.92 (s, 6 H, CH_3) ppm. ^{13}C NMR (75 MHz, $CDCl_3$, 22 °C): δ = 185.4, 132.3, 129.4, 121.6, 21.7 ppm. ^{11}B NMR (128 MHz, $CDCl_3$, 22 °C): δ = 0.54 (t, $J_{B\text{-}F}$ = 30.0 Hz) ppm. ^{19}F NMR (376 MHz, $CDCl_3$, 22 °C): δ = –129.0 (q, $J_{B\text{-}F}$ = 30.0 Hz) ppm. Other characterization can be found in Table 2 and Table 3. Crystals suitable for single-crystal X-ray diffraction were grown by slow cooling of a methanol solution.

BF_2(Me^{4BrPh},H, Ph^{4BrPh}): A mixture of H(Me^{4BrPh},H, Ph^{4BrPh}) (0.19 g, 0.41 mmol) and BF_3·OEt_2 (0.058 g, 0.41 mmol) afforded 0.18 g (85 % yield) of BF_2(Me^{4BrPh},H, Ph^{4BrPh}) as a yellow solid; m.p. 201–202 °C. $C_{22}H_{17}BBr_2F_2N_2$ (518.01): calcd. C 51.01, H 3.31, N 5.41; found C 50.76, H 3.02, N 5.53. ^{1}H NMR (300 MHz, $CDCl_3$, 22 °C): δ = 7.56 (part of AA'BB', *J* = 8.5 Hz, 2 H, aniline), 7.32–7.16 (m, 9 H, Ph, aniline), 6.98 (part of AA'BB', *J* = 8.5 Hz, 2 H, aniline), 5.45 [s, 1 H, -C(N)C*H*C(N)-], 2.02 (s, 3 H, -CH_3) ppm. ^{13}C NMR (75 MHz, $CDCl_3$, 22 °C): δ = 132.4, 131.6, 129.8, 129.5, 129.2, 129.0, 128.5, 121.8, 120.1, 98.2, 21.9, (CN not obsd.) ppm. ^{11}B NMR (128 MHz, $CDCl_3$, 22 °C): δ = 0.89 (t, $J_{B\text{-}F}$ = 30.0 Hz) ppm. ^{19}F NMR (376 MHz, $CDCl_3$, 22 °C): δ = –128.2 (q, $J_{B\text{-}F}$ = 30.0 Hz) ppm. Other characterization can be found in Table 2 and Table 3.

Supporting Information (see also the footnote on the first page of this article): Characterization data for known difluoroboron diketonates, details of X-ray crystallographic studies, tables of X-ray data, details of computational studies, frontier orbital diagrams. The supplementary crystallographic data for this paper are contained in CCDC-CCDC-678449 http://www.ccdc.cam.ac.uk/cgi-bin/catreq.cgi [for BF_2(*t*Bu,H,*t*Bu)], -CCDC-678673 http://www.ccdc.cam.ac.uk/cgi-bin/catreq.cgi [for BF_2(*t*Bu,H,*t*Bu^{Ph})], -CCDC-678674 http://www.ccdc.cam.ac.uk/cgi-bin/catreq.cgi [for BF_2(*t*Bu^{Ph},H,*t*Bu^{Ph})], -CCDC-678450 http://www.ccdc.cam.ac.uk/cgi-bin/catreq.cgi [for BF_2(Me,H,Me^{BrPh})], -CCDC-678669 http://www.ccdc.cam.ac.uk/cgi-bin/catreq.cgi [for BF_2(Me^{BrPh},H,Me^{BrPh})],-CCDC-678447 http://www.ccdc.cam.ac.uk/cgi-bin/catreq.cgi [for BF_2(Ph,H,Ph^{Ph})], -CCDC-678448 http://www.ccdc.cam.ac.uk/cgi-bin/catreq.cgi [for BF_2(Ph,H,Ph^{4BrPh})],-CCDC-678670 http://www.ccdc.cam.ac.uk/cgi-bin/catreq.cgi [for BF_2(Ph,H,Ph^{2BrPh})], -CCDC-678668 http://www.ccdc.cam.ac.uk/cgi-bin/catreq.cgi [for BF_2(Ph,H,Ph^{4pzPh})], -CCDC-678671 http://www.ccdc.cam.ac.uk/cgi-bin/catreq.cgi [for BF_2(Ph,H,Ph^{2pz4tolyl})], -CCDC-678672 http://www.ccdc.cam.ac.uk/cgi-bin/catreq.cgi [for BF_2(Ph,Ph,Ph^{BrPh})], and -CCDC-678667 http://www.ccdc.cam.ac.uk/cgi-bin/catreq.cgi [for BF_2(*p*Anis,H,*p*Anis^{BrPh})]. These data can be obtained free of charge from The Cambridge Crystallographic Data Centre via www.ccdc.cam.ac.uk/data_request/cif.

Acknowledgements

J. R. G. thanks Marquette University and the Petroleum Research Fund for financial support.

References

1 1a R. C. Mehrotra , R. Bohra , D. P. Gaur in *Metal β-Diketonates and Allied Derivatives*, Academic Press, New York, 1978 . 1b L. Bourget-Merle , M. F. Lappert , J. R. Severn , *Chem. Rev.* 2002 , **102** , 3031 – 3065 .

2 Select Examples: 2a K. M. Smith , *Organometallics* 2005 , **24** , 778 – 784 . 2b J. M. Smith , A. R. Sadique , T. R. Cundari , K. R. Rodgers , G. Lukat-Rodgers , R. J. Lachicotte , C. J. Flaschenreim , J. Vela , P. L. Holland , *J. Am. Chem. Soc.* 2006 , **128** , 756 – 769 . 2c Y. M. Badiei , A. Krishnaswamy , M. M. Melzer , T. H. Warren , *J. Am. Chem. Soc.* 2006 , **128** , 15056 – 15057 . 2d Z. J. Tonzetich , A. J. Jiang , R. R. Shrock , P. Muller , *Organometallics* 2006 , **25** , 4725 – 4727 .

3 For instance: 3a A. H. Cowley , Z. Lu , J. N. Jones , J. A. Moore , *J. Organomet. Chem.* 2004 , **689** , 2562 – 2564 . 3b D. Vidovic , J. A. Moore , J. N. Jones , A. H. Cowley , *J. Am. Chem. Soc.* 2005 , **127** , 4566 – 4567 . 3c S. Singh , H.-J. Ahn , A. Stasch , V. Jancik , H. W. Roesky , A. Pal , M. Biadene , R. Herbst-Irmer , M. Noltemeyer , H. G. Schmidt , *Inorg. Chem.* 2006 , **45** , 1853 – 1860 . 3d Y. Yang , T. Schulz , M. John , Z. Yang , V. M. Jimenez-Perez , H. W. Roesky , P. M. Gurubasavaraj , D. Stalke , H. Ye , *Organometallics* 2008 , **27** , 769 – 777 .

4 N. M. D. Brown , P. Bladon , *J. Chem. Soc. A* 1969 , 526 – 532 .

5a Y. P. Singh , P. Rupani , A. Singh , A. K. Rai , R. C. Mehrotra , R. D. Rodgers , J. L. Atwood , *Inorg. Chem.* 1986 , **25** , 3076 – 3081 . 5b K. Itoh , K. Okazaki , M. Fujimoto , *Aust. J. Chem.* 2003 , **56** , 1209 – 1214 .

6 N. Kuhn , A. Kuhn , J. Lewandowski , M. Spies , *Chem. Ber.* 1991 , **124** , 2197 – 2201 .

7 N. Kuhn , A. Kuhn , R. Boese , N. Augart , *J. Chem. Soc., Chem. Commun.* 1989 , 975 – 976 .

8 8a Y. L. Chow , C. I. Johansson , Y.-H. Zhang , R. Gautron , L. Yang , A. Rassat , S.-Z. Yang , *J. Phys. Org. Chem.* 1996 , **9** , 7 – 16 . 8b R. L. Belford , A. E. Martell , M. Calvin , *J. Inorg. Nucl. Chem.* 1956 , **2** , 11 – 31 .

9 9a K. Itoh , K. Okazaki , A. Sera , Y. L. Chow , *J. Chem. Soc., Chem. Commun.* 1992 , 1608 – 1609 . 9b K. Itoh , M. Fujimoto , M. Hashimoto , *New J. Chem.* 2002 , **26** , 1070 – 1075 . 9c K. Itoh , K. Okazaki , Y. Toyotomi , *Heterocycles* 2002 , **57** , 2065 – 2079 . 9d K. Itoh , K. Okazaki , Y. L. Chow , *Helv. Chim. Acta* 2004 , **87** , 292 – 302 .

10 10a G. Haucke , P. Czerney , H. G. Ilge , D. Steen , H. Hartmann , *J. Mol. Struct.* 1990 , **219** , 411 – 416 . 10b Y. L. Chow , C. J. Johansson , *J. Phys. Chem.* 1995 , **99** , 17566 – 17572 . 10c Y. L. Chow , S.-S. Wang , C. I. Johansson , Z.-L. Liu , *J. Am. Chem. Soc.* 1996 , **118** , 11725 – 11732 .

11 For instance, O. T. Beachley Jr , J. R. Gardinier , M. R. Churchill , *Organometallics* 2000 , **19** , 4544 – 4549 .

12 12a P. S. Bailey , T. M. Ferrell , *J. Org. Chem.* 1981 , **46** , 5028 – 5030 . 12b A. Padwa , T. Brookhart , *J. Org. Chem.* 1979 , **44** , 4021 – 4030 .

13 R. Knorr , A. Weiss , *Chem. Ber.* 1981 , **114** , 2104 – 2115 .

14 R. Knorr , A. Weiss , *Chem. Ber.* 1982 , **115** , 139 – 160 .

15 CSD registration number IHEDUU: A. G. Mirochnik , B. V. Bukvetsky , E. V. Gukhman , P. A. Zhikhareva , V. E. Karasev , *Zh. Obshch. Khim.* 2002 , **72** , 737 – 740 .

16 CSD registration number BZACBF: A. W. Hanson , E. W. Macaulay , *Acta Crystallogr., Sect. B* 1972 , **28** , 1961 – 1967 .

17 CSD registration number BOHFUZ: B. Qian , S. W. Baek , M. R. Smith III , *Polyhedron* 1999 , **18** , 2405 – 2414 .

18 CSD registration number XOCJOO: A. G. Mirochnik , B. V. Bukvetsky , E. V. Gukhman , P. A. Zhikhareva , V. E. Karasev , *Izv. Akad. Nauk SSSR , Ser. Khim.* 2001 , **50** , 1612 – 1615 .
19 19a CSD registration number SANKUO: A. G. Mirochnik , B. V. Bukvetskii , E. V. Fedorenko , V. E. Karasev , *Russ. Chem. Bull.* 2004 , **53** , 291 – 296 . 19b E. Cogné-Laage , J.-F. Allemand , O. Ruel , J.-B. Baudin , V. Croquette , M. Blanchard-Desce , L. Jullien , *Chem. Eur. J.* 2004 , **10** , 1445 – 1455 .
20 CSD registration number JENLOD: N. Kuhn , A. Kuhn , M. Speis , D. Blaser , R. Boese , *Chem. Ber.* 1990 , **123** , 1301 – 1306 .
21 CSD YALLIH: K.-H. Park , W. J. Marshall , *J. Org. Chem.* 2005 , **70** , 2075 – 2081 .
22 F. Grepioni , G. Cojazzi , S. M. Draper , N. Scully , D. Braga , *Organometallics* 1998 , **17** , 296 – 307 .
23 H. Nöth , B. Wrackmeyer in *Nuclear Magnetic Resonance Spectroscopy of Boron Compounds*, Springer-Verlag, New York, 1978 .
24 24a N. N. Shapet'ko , L. N. Kurkovskaya , V. G. Medvedeva , A. P. Skoldinov , L. K. Vasyanina , *Zh. Strukt. Khim.* 1969 , **10** , 936 – 942 . 24b J. Bacon , R. J. Gillespie , J. W. Quail , *Can. J. Chem.* 1963 , **41** , 3063 – 3069 .
25 B. J. Liddle , R. M. Silva , T. J. Morin , F. P. Macedo , R. Shukla , S. V. Lindeman , J. R. Gardinier , *J. Org. Chem.* 2007 , **72** , 5637 – 5646 .
26 M. M. Khodaei , A. R. Khosropour , M. Kookhazadeh , *Can. J. Chem.* 2005 , **83** , 209 – 212 .
27 E. E. Turner , *J. Chem. Soc. Trans.* 1917 , **111** , 1 – 4 .
28 D. F. Martin , G. A. Janusonis , B. B. Martin , *J. Am. Chem. Soc.* 1961 , **83** , 73 – 75 .
29 J. Grimshaw , A. P. De Silva , *J. Chem. Soc. Perkin Trans. 2* 1981 , 1010 – 1014 .
30 S. Sahoo , *J. Mol. Catal. A* 2006 , **244** , 179 – 182 .